TRACE CONTAMINANT CONTROL: AN IN-DEPTH STUDY OF A SILICA-TITANIA COMPOSITE FOR PHOTOCATALYTIC REMEDIATION OF CLOSED-ENIVRONMENT HABITAT AIR

by

JANELLE L. COUTTS
B.S. University of Central Florida, 2008

A dissertation submitted in partial fulfillment of the requirements
for the degree of Doctor of Philosophy
in the Department of Chemistry
in the College of Sciences
at the University of Central Florida
Orlando, Florida

Spring Term
2013

Major Professor: Cherie L. Yestrebsky

ABSTRACT

This collection of studies focuses on a PCO system for the oxidation of a model compound, ethanol, using an adsorption-enhanced silica-TiO_2 composite (STC) as the photocatalyst; studies are aimed at addressing the optimization of various parameters including light source, humidity, temperature, and possible poisoning events for use as part of a system for gaseous trace-contaminant control system in closed-environment habitats.

The first goal focused on distinguishing the effect of photon flux (i.e., photons per unit time reaching a surface) from that of photon energy (i.e., wavelength) of a photon source on the PCO of ethanol. Experiments were conducted in a bench-scale annular reactor packed with STC pellets and irradiated with either a UV-A fluorescent black light blue lamp (λ_{max}=365 nm) at its maximum light intensity or a UV-C germicidal lamp (λ_{max}=254 nm) at three levels of light intensity. The STC-catalyzed oxidation of ethanol was found to follow zero-order kinetics with respect to CO_2 production, regardless of the photon source. Increased photon flux led to increased EtOH removal, mineralization, and oxidation rate accompanied by lower intermediate concentration in the effluent. The oxidation rate was higher in the reactor irradiated by UV-C than by UV-A (38.4 vs. 31.9 nM s^{-1}) at the same photon flux, with similar trends for mineralization (53.9 vs. 43.4%) and reaction quantum efficiency (i.e., photonic efficiency, 63.3 vs. 50.1 nmol CO_2 μmol photons^{-1}). UV-C irradiation also led to decreased intermediate concentration in the effluent compared to UV-A irradiation. These results demonstrated that STC-catalyzed oxidation is enhanced by both increased photon flux and photon energy.

The effect of temperature and relative humidity on the STC-catalyzed degradation of ethanol was also determined using the UV-A light source at its maximum intensity. Increasing

temperature from 25°C to 65°C caused a significant decrease in ethanol adsorption (47.1% loss in adsorption capacity); minimal changes in EtOH removal; and a dramatic increase in mineralization (37.3 vs. 74.8%), PCO rate (25.8 vs. 53.2 nM s^{-1}), and reaction quantum efficiency (42.7 vs. 82.5 nmol CO_2 μmol $photons^{-1}$); intermediate acetaldehyde (ACD) evolution in the effluent was also decreased. By elevating the reactor temperature to 45°C, a ~32% increase in reaction quantum efficiency was obtained over the use of UV-C irradiation at room temperature; this also allowed for increased energy usage efficiency by utilizing both the light and heat energy of the UV-A light source. Higher relative humidity (RH) also caused a significant decrease (16.8 vs. 6.0 mg EtOH g $STCs^{-1}$) in ethanol adsorption and dark adsorption 95% breakthrough times (48.5 vs.16.8 hours). Trends developed for ethanol adsorption correlated well with studies using methanol as the target VOC on a molar basis. At higher RH, ethanol removal and ACD evolution were increased while mineralization, PCO rate, and reaction quantum efficiency were decreased. These studies allowed for the development of empirical formulas to approximate EtOH removal, PCO rate, mineralization, and ACD evolution based on the parameters (light intensity, temperature, and RH) assessed.

Poisoning events included long-term exposure to low-VOC laboratory air and episodic spikes of either Freon 218 or hexamethylcyclotrisiloxane. To date, all poisoning studies have shown minimal (0-6%) decreases in PCO rates, mineralization, and minimal increases in ACD evolution, with little change in EtOH removal. These results, while studies are still ongoing, show great promise of this technology for use as part of a trace contaminant control system for niche applications such as air processing onboard the ISS or other new spacecrafts.

ACKNOWLEDGMENTS

I would first like to thank several crucial members from the Engineering Services Contract (ESC) at Kennedy Space Center for their support throughout this project: Dr. Lanfang Levine for giving me the opportunity to work at the Space Life Sciences Lab, encouraging me to strive for greatness, and for irreplaceable guidance in project planning and data interpretation; Mr. Jeffrey Richards for teaching me so many laboratory techniques and support in assisting in experimental data collection and processing; Mr. Lawrence Koss for his exceptional assistance with the construction of the photocatalytic test bed and OPTO 22 data logging software maintenance, without which the project could not have been completed; and finally, Dr. Paul Hintze, Phil Maloney, and Dr. Steve Trigwell for assistance with the SEM and XPS analysis of the catalyst. I would also like to thank Dr. Ray Wheeler from NASA for his agreement to support me as part of my doctoral committee on such short notice.

Furthermore, I would like to extend my gratitude to my co-advisors, Dr. Cherie Yestrebsky and Dr. Christian Clausen, for their continued support and belief in me throughout my graduate career and to my other committee members, Dr. Seth Elsheimer and Dr. Michael Sigman for their time in supporting me. My lab mates both in the Industrial Chemistry Laboratory at UCF and throughout NASA-KSC have given much needed support through their friendship and encouragement over the years. Finally, I could not have gotten this far without the support from my mother, stepfather, grandparents, and my loving husband, William Dorner, who has always believed in my dreams.

TABLE OF CONTENTS

LIST OF FIGURES

LIST OF TABLES

LIST OF ACRONYMNS, ABBREVIATIONS, AND SYMBOLS

ACD – Acetaldehyde

c – Speed of Light

CFC - Chlorofluorocarbon

$[CO_2]_{OUT}$ – CO_2 Generated from PCO

E – Energy

EDX – Energy-Dispersive X-Ray Spectroscopy

EPA – Environmental Protection Agency

ESC – Engineering Services Contract

EtOH – Ethanol

$[EtOH]_{IN}$ – Influent EtOH Concentration

$[EtOH]_{OUT}$ – Effluent EtOH Concentration

GC-FID – Gas Chromatograph-Flame Ionization Detector

GC-MS – Gas Chromatograph-Mass Spectrometer

h – Planck's Constant

I.D. – Inner Diameter

KSC – Kennedy Space Center

λ – Wavelength

λ_{max} – Maximum Wavelength

LED – Light Emitting Diode

MeOH – Methanol

NASA – National Aeronautics and Space Administration

O.D. – Outer Diameter

PCO – Photocatalytic Oxidation

φ – Photon Flux

ppm_v – Parts per Million (by Volume)

PVC – Polyvinyl chloride

r – PCO Rate

RH – Relative Humidity

Rxn - Reaction

SEM – Scanning Electron Microscope

SPME – Solid Phase Micro-Extraction

STC – Silica-Titania Composite

TCE - Trichloroethylene

TPD – Temperature-Programmed Desorpsion

TPO – Temperature-Programmed Oxidation

UV – Ultraviolet

UV-A BLB – UV-A Blacklight Blue Lamp

UV-C GL – UV-C Germicidal Lamp

VOC – Volatile Organic Compound

W.D. – Working Distance

X_A – Mineralization Efficiency

XPS – X-ray Photoelectron Spectroscopy

ξ – Photonic Efficiency/Reaction Quantum Efficiency

CHAPTER ONE: INTRODUCTION

The increasing awareness of health risks associated with poor air quality in closed-environment habitats (e.g., airplanes, spacecrafts, office buildings, factories, homes, etc.) as well as the increasing desire for energy conservation have provoked a high demand for more efficient and environmentally-friendly technologies for air revitalization. The current technology uses two major types of air purification units; the first category includes units based on filters to remove particulate matter or a sorbent material to collect gases and odors while the second category utilizes thermal oxidation whereby trace contaminants are broken down by heat with or without the assistance of a catalyst. While effective at the removal of volatile organic compounds (VOCs), these methods both have their own shortcomings. Sorbent materials and filters only trap the contaminants and must undergo further handling and disposal procedures to render the contaminants nonhazardous; they also require replacement or refurbishment after the material is spent[1, 2]. On the other hand, thermal methods act to break down contaminants but require significant energy input for heating: temperatures in the range of 200-250°C for processes incorporating catalysts[3] and a range of 730-850 °C for those processes not incorporating catalysts[4]; furthermore, there is the potential for harmful side-product formation (e.g., NO_x and SO_2) from the thermal processes, requiring subsequent purification[5]. An emerging alternative method for air pollution control employs the use of semiconductors in photocatalytic oxidation (PCO) of organic contaminants to produce innocuous CO_2 and H_2O[1, 6, 7]. The primary advantages of PCO over the aforementioned technologies are the use of non-expendable materials and low energy demand because the process can operate at or near room temperature[8]. This collection of studies focuses on a PCO system for the oxidation of a model

compound, ethanol, using an adsorption-assisted silica-titania composite (STC) catalyst; studies are aimed at addressing various parameters including choice of light source, humidity, and temperature, as well as assessing possible catalyst poisoning events for the optimization of the reactor system for use as a trace-contaminant control system in closed-environment habitats.

The Photocatalytic Process

In the photocatalytic process, light acts as an excitation source to promote an electron from the valence band to the conduction band, generating an electron-hole pair in the semiconductor catalyst. The electron and hole then participate in the reduction and oxidation of the contaminant species in a series of radical reactions[9] or recombine[10] as seen in Figure 1. The amount of energy required to produce the electron-hole pair is known as band-gap energy; when this energy is known, the corresponding wavelength of light can be derived from the Planck-Einstein Equation, $E=hc/\lambda$.

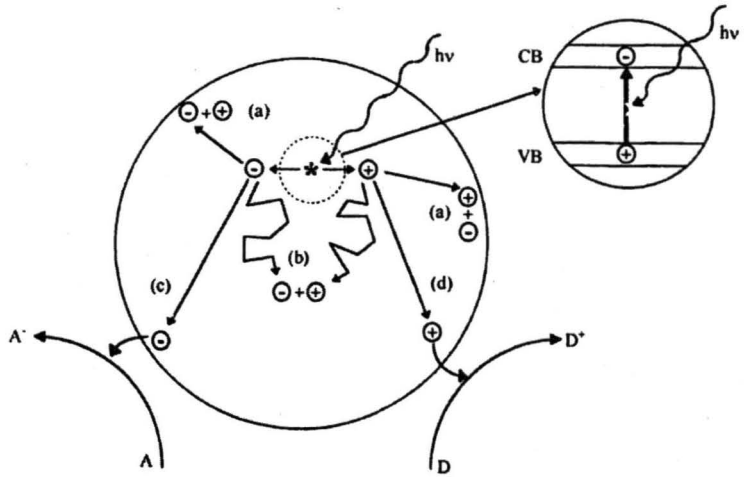

Figure 1: Major processes occurring after excitation of electron in photocatalysis according to Mills and Le Hunte[10]. Electron-hole recombination can occur at the surface (a) or in the bulk (b) of the semiconductor, electrons can participate in reduction reactions (c), and holes can participate in oxidation reactions (d).

Among the photocatalysts used, titanium dioxide (TiO_2) is the most widely implemented because it is inexpensive, nonhazardous, and chemically inert. Commercially available nanoparticle TiO_2, known as Degussa P25, is a simple mixture of anatase (70-85%), rutile, and amorphous (minor) titania[11] and has demonstrated high PCO activity in numerous studies[9, 12-16]. The anatase phase is known for its superiority in photocatalytic activity over the rutile phase[17]. The band gap energy of anatase TiO_2 is 3.2 eV; thusly, a light source with a wavelength below 388 nm has sufficient energy to activate the anatase TiO_2[8].

Heterogeneous Photocatalytic Oxidation (PCO) of Ethanol

Degradation pathways and kinetics of heterogeneous photocatalytic systems have been studied by several groups in order to better understand intermediate formation and adsorption on the catalyst surface. Sauer and Ollis[18] studied the mechanism of the PCO of ethanol in a batch-type reactor, determining the reaction pathway to proceed as follows: ethanol oxidizes to acetaldehyde, acetaldehyde to a mixture of formaldehyde and CO_2, and formaldehyde to CO_2. Similarly, Nimlos et al[19] used a batch-type reactor for studying the same pathway and determined it to proceed slightly differently where acetaldehyde oxidizes to acetic acid, acetic acid to formaldehyde, and formaldehyde to a mixture of formic acid and CO_2 before total mineralization of all products to carbon dioxide. They also discuss the importance of O_2 species in the PCO of ethanol. More recently, Muggli et al[20] studied the same reaction in a transient-type reactor to study what intermediates may still be adsorbed to the catalyst surface after the PCO is ended. By utilizing a temperature-programmed desorbsion (TPD) process, they proposed a mechanism that includes parallel reaction pathways.

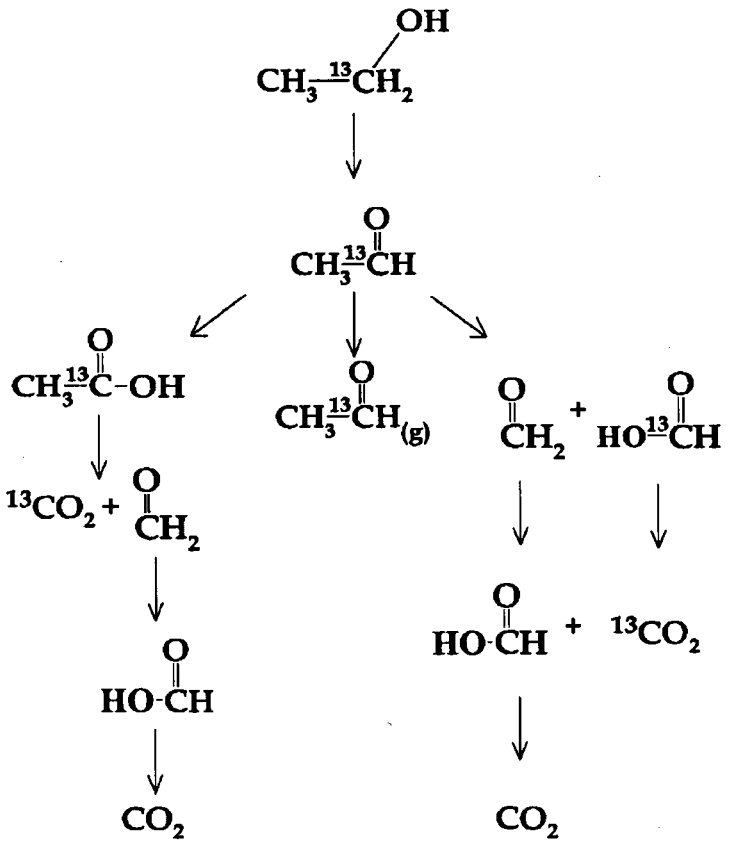

Figure 2: Mechanism of the photocatalytic oxidation of ethanol according to Muggli et al.[20]

Based on their PCO, TPD, and temperature-programmed oxidation (TPO) studies, the reaction mechanism in Figure 2 was developed. Upon UV irradiation, a portion of the adsorbed ethanol was seen to form acetaldehyde (some of which desorbs at room temperature)[20]. The acetaldehyde that remained on the surface was proposed to react by two parallel pathways to form either acetic acid or a formic acid/formaldehyde mixture. Muggli et al[20] determined that the acetic acid oxidizes to CO_2 (α-carbon) and to CO_2 through formaldehyde and formic acid intermediates (β-carbon) using ^{13}C-labelled acetic acid[20]. The formaldehyde formed directly from the acetaldehyde followed a similar oxidation to CO_2 through a formic acid intermediate.

The studies were completed under low and atmospheric O_2 concentrations and also in the absence and presence of water. The reaction pathway was found to be the same in all cases, but the percentage of ethanol following each pathway varied with water and O_2 concentrations[20].

Photon Sources for Photocatalysis

UV light sources of various wavelengths ranging between 250-400 nm, and with various intensities, have been used in TiO_2-catalyzed photocatalysis[1, 13, 21-25]. Studies by Stokke et al[13], Dijkstra et al[21], Cen et al[22], Alberci and Jardin[23], Kim and Hong[24], and Jacboy[25] reported that a UV-C-irradiated (λ_{max} = 254 nm) reactor resulted in greater photocatalytic oxidation of VOCs than a reactor irradiated with UV-A light (λ_{max} = 365 nm), implying that a shorter wavelength light source (i.e., higher energy photons) is more efficient. However, interpretation of the results from these studies on the effect of wavelength on TiO_2-assisted photocatalysis is confounded with the influence of light intensity as these studies were conducted either at different light intensities or the light intensity was not well defined. It is well known that UV light intensity received at the catalyst surface dramatically affects oxidation rates[1, 15, 26], but a more clear understanding of its effects needs to be addressed. Furthermore, there are discrepancies in the literature regarding whether the use of UV-A or UV-C light sources results in the formation of more intermediates. Although Grela and Colussi[26] clearly demonstrated that the reaction quantum yield for the photocatalytic oxidation of 3-nitrophenol in aerated, aqueous colloids of crystalline or metastable TiO_2 nanoparticles was a function of photon wavelength ($254 \leq \lambda/nm \leq 366$), no similar data was available for gas-phase photocatalysis. Distinguishing the effect of UV wavelength from that of UV light intensity has profound implications in the design of an energy-efficient and low-risk PCO reactor for the

following two reasons: 1) despite the higher lighting efficiency of current UV-C lamps over that of UV-A lamps, UV-C radiation is more damaging and can cause serious skin and eye injuries from both direct and reflected radiation, and 2) both traditional UV-A and UV-C lamps contain a trace amount of highly toxic and EPA-regulated mercury; light emitting diodes (LEDs) are a promising alternate light source and lighting efficiency increases with longer wavelength LED devices (~350 nm)[27]. Therefore, the one objective of this study is to distinguish the effect of photon flux (i.e., light intensity) from that of photon energy (i.e., wavelength) by exploring the photocatalytic degradation of ethanol in the gas phase by an adsorption-enhanced TiO_2 photocatalyst (silica-titania composites, STCs)[14] under the illumination of UV-C and UV-A sources. Experiments were conducted in the same reactor, and the UV-C lamp was attenuated to obtain a range of photon fluxes that brackets that of the UV-A lamp.

Temperature Effects on Photocatalysis

Many heterogeneous photocatalytic studies have utilized aqueous solutions at ambient temperatures. It has generally been seen that increasing the reaction temperature improves PCO rates for liquid phase reactions over a range of 20-60°C[28]. However, temperature effects on PCO in the gas phase have not been widely investigated[28-30]. Blake and Griffin[29] studied the PCO of 1-butanol, determining that the maximum PCO rate occurred at 107°C before beginning to decrease at higher temperatures. Complete mineralization of trichloroethylene was found to occur at 64°C according to Anderson et al[28, 31] while Pichat et al[30] cited that the PCO of propene decreased with increasing temperature. Fu et al[28] further studied the PCO of ethylene over a temperature range of 30-110°C at various humidity levels; it was determined that the PCO rate of mineralization of ethylene increased with increasing temperature regardless of

the humidity level, but the water content also played a crucial role in the efficiency of the reaction. No appreciable oxidation of ethylene was seen over the entire temperature range when no light was present indicating that the mineralization of ethylene was not due to thermal catalytic oxidation, but was indeed due to photocatalytic oxidation throughout their studies[28]. Westrich et al[32] similarly studied the high-temperature PCO of ethylene over a temperature range of 60°C to 520°C in order to investigate charge carrier recombination dynamics. They determined that all catalysts studied (TiO_2 catalysts with varied anatase/rutile composition) exhibited an exponential increase in thermally oxidized ethylene with increased temperature; the addition of UV photons contributed to ethylene conversion at low to moderate temperatures (< 325°C) but had a diminishing effect. The maximum ethylene oxidation rates occurred between 100°C and 200°C[32], slightly higher than the range tested by Fu et al[28]. Westrich et al explained that the loss in photocatalytic activity at high temperatures could be attributed to the loss of surface hydroxyl groups or photogenerated charge carriers; further experimentation supported the loss of photogenerated charge carriers rather than the loss of hydroxyl radicals[32].

It is obvious that for various test contaminants and catalysts, temperature can be used to optimize the efficiency of the oxidation reaction. Experiments outlined in the current studies determine the temperature effects on the STC-catalyzed PCO of ethanol and were completed using UV-A irradiation over the range of 25-65°C. Furthermore, Fu et al[28] propose that energy utilization in the majority of PCO processes is inefficient because all lamps transform electrical energy into light as well as heat. For instance, according to manufacturer specifications for a Phillips 40W fluorescent lamp emitting light at a peak wavelength of 350 nm, only 21% of the input electrical energy is converted to UV light, leaving approximately 79% of

the input energy being converted to heat[28]. As mentioned above, most PCO reactions are carried out at ambient temperatures (often by cooling the reaction apparatus to remove the heat produced by the light source). Thus nearly all thermal energy produced by the light source is being wasted rather than being utilized to help drive PCO reactions. This theory was applied to the work completed for the included temperature experiments to determine whether the heat evolved from the light source can benefit the PCO reaction.

The Role of Water in PCO Rates

Another crucial parameter in photocatalytic degradation reactions is the concentration of water vapor in the system. Multiple studies on various target VOCs have found that water affects PCO rates in different ways; it has been seen to possess both activating and inhibitory characteristics which are heavily dependent on the target compound in the photocatalytic oxidation reaction. According to Stavrakakis et al[33], water vapor has been seen to react in PCO systems via two main phenomena: 1) water molecules can be transformed into hydroxyl radicals which are adsorbed at the titania surface leading to higher reaction rates or 2) water molecules undergo competitive adsorption with the target VOC molecules on the titania surface and can lead to lower reaction rates if the VOC cannot reach any active sites. Since, in real-world applications, most PCO reactions would occur in humid environments, it is essential to understand how water content in the specific matrix being implemented.

Ibusuki and Tekeuchi[34] studied the effect of water vapor on the photocatalytic oxidation of toluene over a UV-irradiated TiO_2 catalyst; it was determined in their studies that increasing the RH from 0% to 60% significantly increased the oxidation rate. This increase was attributed to the possibility of an increase in hydroxyl radical formation at the higher humidity

level[34]. Stavrakakis et al[33] also studied the effect of humidity on toluene over two separate catalysts, Degussa P25 deposited on a glass substrate and an anatase TiO_2-SiO_2 hybrid. As humidity was increased, the Degussa P25 catalyst exhibited a lower adsorption capacity but higher reaction rate while the TiO_2-SiO_2 catalyst experienced lower adsorption capacity and oxidation rate capacity for toluene[33]. Furthermore, the profile of intermediates detected during the reaction changed with humidity levels similar to the trend described for ethanol by Muggli et al[20] showing that the degradation pathway is also dependent on water content.

Studies focused on the photocatalytic oxidation of trichloroethylene (TCE)[24, 35] over a range of humidity levels generally found that increasing water content inhibited the oxidation rate of the contaminant. The decrease was attributed either to the competitive adsorption of water and TCE on the catalyst surface[24] or the possible suppression of the chlorine atom-propagated chain reaction involved in the PCO mechanism of TCE[35]. Fu et al[28] also attributed the impedance of the PCO of ethylene with increasing humidity at low temperatures to the competitive adsorption between the target compound and water, but were able to recover oxidation capacity by increasing the temperature of the system. Further studies by Peral and Ollis[36] found that acetone oxidation was inhibited by increasing humidity and that the oxidation of 1-butanol was unaffected[36]. In the same study, it was determined that *m*-xylene was seen to have an increasing oxidation rate from 0% to 2.5% RH after which a decrease in activity was seen[36]. This variable role was explained by the possibility of the need for trace water to achieve oxidation activity, but that excess water would cause a decrease in activity due to adsorption competition[36].

As seen by the plethora of varied results, water vapor content can play an important role in the efficiency of gas-phase PCO reactions and its function in photocatalytic oxidation reactions is heavily dependent on the target compound. There is an obvious balance between its ability to enhance reaction rates by providing an increasing concentration of hydroxyl radicals available and its undesirable effect of lowering reactivity due to its adsorption specificity for the PCO catalyst. While Muggli et al[20] outlined that the degradation pathway of the photocatalytic oxidation of ethanol is altered by varying humidity, little was mentioned on the dependence of oxidation rate; this need, coupled with the use of an unique adsorption-assisted catalyst in the current studies, warrants further investigation of this parameter for the optimization and understanding of this PCO system.

Catalyst Poisoning

A niche application for PCO technology at NASA-Kennedy Space Center is gas-phase trace contaminant control in closed-habitats such as future spacecrafts, the International Space Station (ISS), etc. Extensive trace contaminant control modeling based on various US space programs has shed light on the major constituents found in cabin air due to metabolic and equipment off-gassing. In-flight cabin air samples from the Space Shuttle and Space Lab Programs revealed that 58 compounds account for 97% of the total trace contaminant load[37] and current contaminant load models list a total of 214 compounds requiring monitoring[37]. Chemical detected on the ISS are split into the following groups: methane, halocarbons, non-methane hydrocarbons, siloxanes, and hydrogen. Non-methane hydrocarbons found in ISS cabin air can be further split into alcohols (79% of non-methane hydrocarbons), aldehydes (7%),

ketones (6%), halocarbons (4%), aromatics (3%), and esters (1%)[37]. Ethanol, the target compound in the present studies, is the most prevalent of alcohols detected.

With any catalytic system, the catalyst must be evaluated for ruggedness including an estimated lifetime at projected operation parameters and susceptibility to possible poisoning agents. Of the major types of catalyst deactivation, chemical poisoning is the most likely mechanism leading to photocatalyst degradation. Of the major constituents identified in ISS cabin air, several compound families are capable of possible deactivation such as siloxanes and halocarbons. Hay et al[38] and Sun et al[39] both investigated the deactivation of TiO_2 by siloxanes. Sun et al[39], while studying the decomposition of octamethyltrisiloxane by PCO, found that with repeated exposure, the TiO_2 catalyst lost activity. Their proposed deactivation mechanism involved the adsorption of hydroxylated SiO_x groups on the catalyst surface, with ~7 monolayers of SiO_x causing complete deactivation[39]. Hay et al[38] similarly correlated TiO_2 deactivation with surface SiO_2 coverage after TiO_2 exposure to tetramethylsilane. Octamethylcyclotetrasiloxane (1.167 mg/m^3), decamethylcyclopentasiloxane (0.827 mg/m^3), and hexamethylcyclotrisiloxane (1.732 mg/m^3) are the three siloxanes nominally found in the ISS atmosphere[40]. The effect of hexamethylcyclotrisiloxane on the unique adsorption-assisted TiO_2 catalyst in this study was investigated due to the ability of siloxanes to have such a damaging effect of the PCO capability of titania.

Halocarbons are also of concern for catalyst detactivation. Several thermal catalytic studies have been completed on the degradation of clorofluorocarbons (CFCs) and fluorocarbons[41, 42] that site deactivation of the catalyst over time. Decomposition studies of dichlorodifluoromethane (CFC-12) over a TiO_2 catalyst by Karmakar and Greene[41] showed

that their catalyst suffered rapid deactivation when the contaminant feed stream contained no water vapor, but activity was uninhibited when water vapor was present. In the absence of water, a semisolid yellowish deposit formed at the reactor exit which solidified and turned white over time; XRD analysis of the solid determined that it was $TiOF_2$[41]. Farris et al[42] found significant deactivation of a Pt/Al_2O_3 catalyst from the degradation of hexafluoropropylene; possible causes were cited as irreversible poisoning of the platinum metal by fluorine adsorption, and degradation of the catalyst support. Little work has been published on photocatalytic systems for the degradation of CFCs and fluorocarbons; while Tennakone and Wijayantha[43] demonstrated a successful photocatalytic system for the destruction of CFC-12 and Sangchakr et al[44] successfully degraded 1,1-difluoroehtane using TiO_2 and UV-C light, neither described any catalyst deactivation studies. While dichloromethane is the most prevalent halocarbon present in ISS cabin air at an average concentration of 0.14 mg/m^3[37], a compound that is not included in model estimates is octafluoropropane (Freon 218). This compound is utilized as a thermal working fluid in the ISS Russian On-orbit Segment (ROS); periodic leaks into the cabin have, at times, resulted in cabin concentrations exceeding 600 mg/m^3[37]. For this reason, Freon 218 was also chosen as a candidate compound to study deactivation effects of halocarbons on the current system.

CHAPTER TWO: METHODS AND MATERIALS

Photocatalyst

Silica-titania composite pellets (STCs) were supplied by Sol Gel Solutions, LLC in the form of 2 mm x 6 mm pellets. The STC was prepared by adding commercially available Degussa P25 TiO_2 to a silica sol derived from the acid hydrolysis of tetraethyl orthosilicate (TEOS). Analysis of the STC by Sol Gel Solutions, LLC showed that the material had a porosity of 30-40Å and contained 4% TiO_2 (4 g Degussa P25 TiO_2 in 100 mL of TEOS silica precursor)[14]. No properties of the Degussa P25 TiO_2 were altered during the STC synthesis process. EDX analysis was completed on a JOEL JSM-7500F Field Emission Scanning Electron Microscope using LEI detection at an 8-mm working distance and demonstrated highly incorporated titania and silica as seen in Figure 3[8].

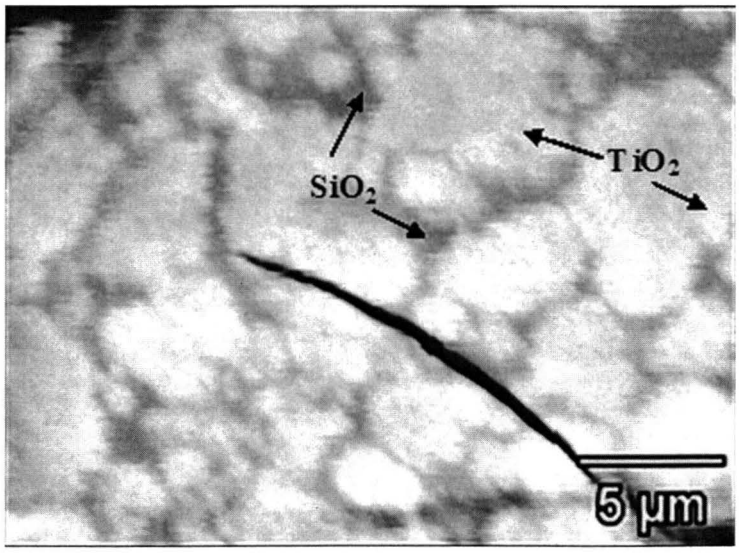

Figure 3: SEM image (5000x magnification, LEI detection, 8-mm W.D.) of a crushed STC pellet; EDX analysis revealed that the white areas corresponded to titania while the dark grey areas corresponded to silica[8].

Light Sources and Characterization

An 8-W UV-A (F8T5) black light blue lamp (UV-A BLB) from Philips (Amsterdam, Netherlands) with dimensions of 15.6 mm (diameter) x 304.8 mm (length) with a radiant output of 1.4 W was selected for all experiments utilizing a UV-A photon source. An 8-W UV-C (G8T5/OF) germicidal lamp (UV-C GL) with 2.5W of radiant output from Sylvania (Danvers, MA) was selected for all experiments utilizing a UV-C photon source. The irradiance profiles at the surface of the catalyst bed for the selected light sources were determined in a dark room (*ex situ*) using a spectroradiometer (model OL754C, Optronics Laboratories, Orlando, FL). The desired light source was centered inside a quartz sleeve (25 mm I.D. and 28 mm O.D.) and placed directly on top of the integrating sphere; light attenuating discs with 12.7-mm and 6.35-mm diameters were used to avoid saturation of the detector during the UV-A and UV-C profiling, respectively[8].

Photocatalytic Oxidation (PCO) Reactor

A custom-built annular reactor (Southern Scientific, Inc., Micanopy, FL) was used in all studies and accommodated both the UV-A and UV-C light source interchangeably (Figure 4). The reactor was comprised of an outer Pyrex housing (38.8 mm I.D. and 42.0 mm O.D.) and an inner quartz sleeve (25 mm I.D. and 28 mm O.D.) with Teflon caps to create an air-tight environment; the total reactor length was 15.24 cm. 3-mm Glass beads were added to allow the STCs to be packed in the center (vertically) of the annular space as well as to assist in air distribution. The STC pellets (14.6 grams) were then packed in the annular space (5 mm) resulting in a bed height of ~65 mm. Temperature was controlled within 0.1°C of the desired set

point for all experiments via a water jacket and thermostated water bath. The light source was centered in the quartz sleeve of the reactor and the entire reactor was shelled by an aluminum-lined PVC housing to avoid penetration of room light into the reactor system as well as to avoid accidental UV exposure of lab personnel[8].

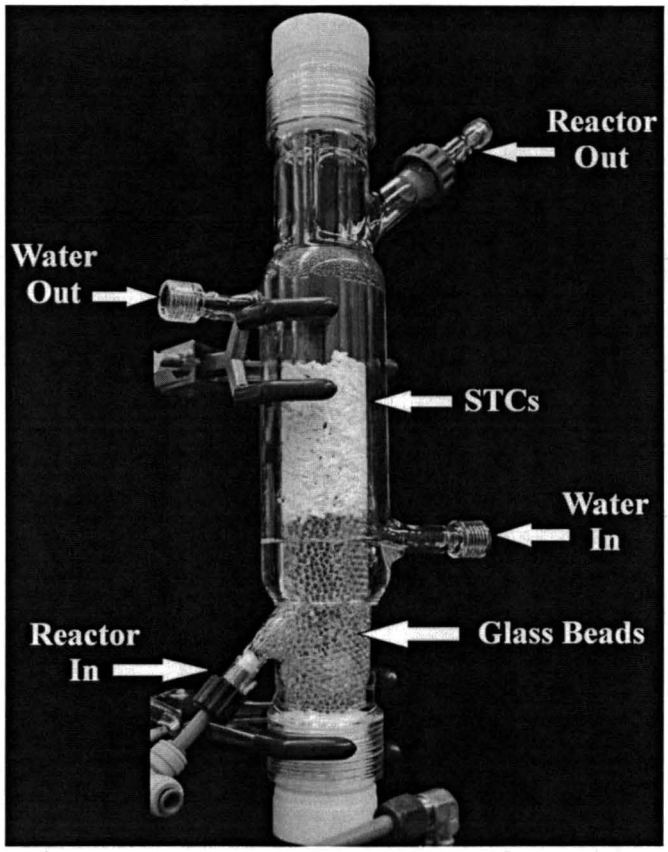

Figure 4: Annular photocatalytic reactor packed with 14.6 g STC pellets as used in all experiments[8].

PCO Experiments and Process Monitoring

Test Bed Setup

All experiments were performed in the annular reactor packed with 14.6 g of STC pellets under illumination of either the UV-A or UV-C source described above. All tests were carried

out, in a flow-through mode with an uninterrupted 2 L min^{-1} CO_2-free air (at a highly-controlled relative humidity, RH) containing 50 ppm_v ethanol (Pharmco-Aaper, Brooksfield, CT) as the test volatile organic compound (VOC) as described previously[15]. The STC pellets were regenerated in-line between each test by passing VOC-free sweeping gas through the reactor accompanied by UV irradiation. Both influent and effluent streams were sampled alternately every 8.45 minutes and analyzed for ethanol and its oxidation intermediates by GC-FID equipped with an HP Plot Q column (30 m x 0.32 mm, 20 μm d.f.). The effluent stream was also directed to a CO_2 analyzer for the determination of the rate of CO_2 production[8]. Data logging of parameters not recorded by the GC/FID software was completed using a custom-programmed OPTO 22 system. Figure 5 is a schematic of the PCO testbed.

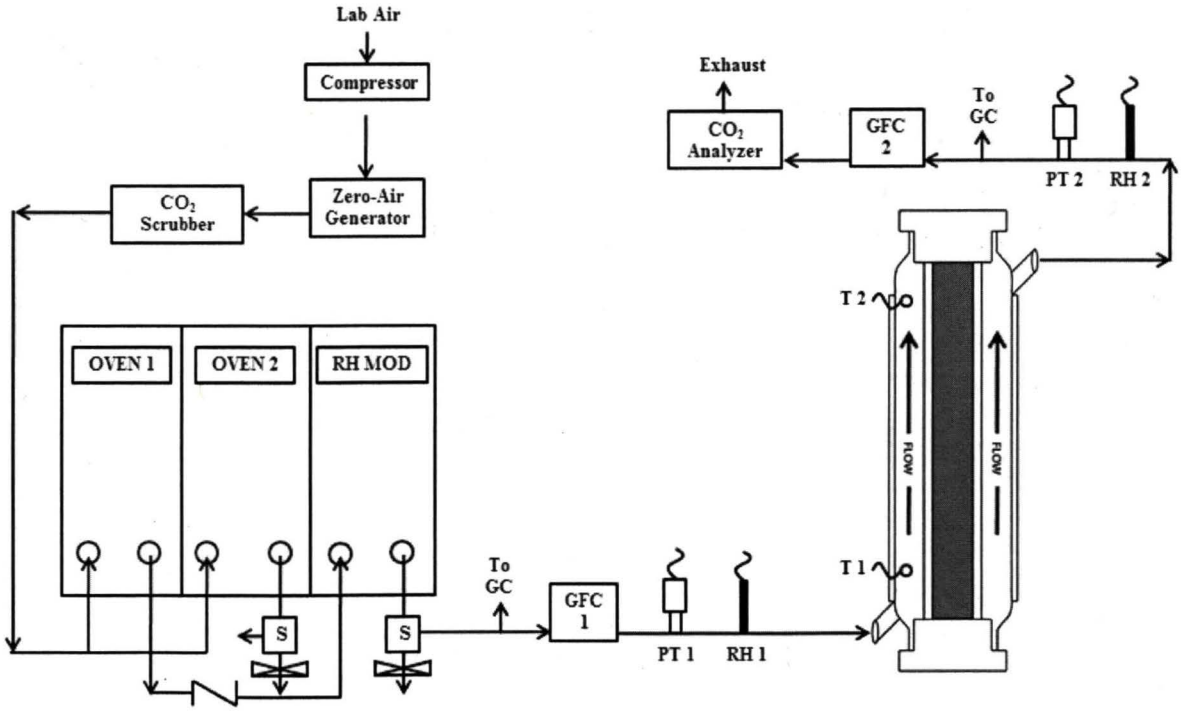

Figure 5: Schematic of PCO testbed setup

Photon Source Studies

The first series of experiments was focused on the effect of photon energy versus that of photon flux on the photocatalytic oxidation of ethanol; the UV-A BLB was used at its maximum light intensity and the UV-C GL was used at three varied intensity levels. The desired UV-C intensity was achieved using a fine stainless-steel mesh (U.S. mesh size 16, referred to hereafter as attenuation mesh) between the quartz sleeve and the lamp as a neutral density filter. The temperature of the reactor was controlled to 25 ± 0.1 °C, and the RH of the gas stream was controlled to 74.7 ± 0.8 % RH. All other parameters as outlined in the test bed setup were followed.

Relative Humidity Studies

A series of experiments using the UV-A BLB photon source and reactor temperature controlled to 25 ± 0.1 °C was completed to determine the effect of humidity on the PCO activity of the silica-titania composite due to the unique adsorptive property of the material. Relative humidity was controlled at 17.2 ± 0.3 %, 46.2 ± 0.4%, and 74.7 ± 0.8% for this RH series. Two types of tests were completed during this study at the varied RHs: 1) determination of the photocatalytic activity differences due to relative humidity and 2) determination of the adsorption capacity of the catalyst at the varied parameters. Type 1 experiments followed all parameters as outlined in the test bed setup. Type 2 experiments for the adsorption capacity studies, followed all parameters outline in the test bed setup were followed with the exception that there was no UV illumination.

Temperature Studies

Similarly to studying the effect of relative humidity on the photocatalytic system, a series of experiments was carried out to determine the effect of temperature on the process using the UV-A BLB photon source and reactor relative humidity controlled to 74.7 ± 0.8 % RH. Temperatures evaluated were 25, 35, 45, and 65 ± 0.1 °C. Both photocatalytic activity (Type 1 experiments) and adsorption capacity (Type 2 experiments) assessments were completed for all temperatures similarly to that completed for the RH series. The adsorption capacity studies also served to evaluate the possibility of thermal catalytic activity occurring in the system.

Catalyst Poisoning Studies

While ethanol was the model VOC studied, several common compounds known to often poison catalysts were introduced to the system as well. After the initial photocatalytic activity of a fresh batch of catalyst was determined for ethanol, the reactor was spiked with one such compound through a gas stream at 2 L min^{-1} for 24 hours; the system was then regenerated as outlined in the test bed setup. Finally, the system was reevaluated using ethanol to determine if there was a decrease and/or change in photocatalytic activity. The catalyst poisoning chemicals evaluated were 0.247 ± 0.038 ppm_v hexamethylcyclotrisiloxane (Sigma Aldrich, St. Louis, MO) and 78.0 ± 0.5 ppm_v Freon 218 (octofluoropropane, Air Liquide, Morrisville, PA).

Beyond assessing the PCO of ethanol after a spike event, the effluent from the reactor during the spike event also analyzed to determine if any of the poisoning chemicals were degraded. Effluent samples were taken directly from the reactor effluent port and analyzed via GC-MS (equipped with an Agilent HP-1 column, 60 m x 0.32 mm x 1μm d.f., and a J&W

Scientific DB624 column, 30 m x 0.32 mm x 1.8 μm d.f., for analysis of the siloxane and Freon 218, respectively). SEM (JEOL SEM as described previously) and XPS (Thermo Scientific K-Alpha) analyses were also completed for catalyst samples before and after the spike events.

The estimated lifetime of the catalyst was also evaluated; similar to the poisoning studies above, the initial photocatalytic activity of a fresh batch of catalyst was determined using ethanol was the target contaminant. The reactor system was then exposed to laboratory air (low-VOC concentration) through a pump at 2 L min^{-1} for periods of two weeks. After each two-week interval, the reactor was evaluated for any changes in photocatalytic activity, again using ethanol as the target VOC. A profile of compounds in the room air was completed using GC-MS (equipped with the previously described Agilent HP-1 column) and a 75-μm Carboxen™/Polydimethylsiloxane SPME air sampling apparatus. Total organic carbon for polar compounds in the laboratory air was assessed by bubbling room air through a set of three pyrex impingers containing e-pure water for 24 hours followed by analysis of the water on a Sievers 5310C Laboratory TOC system.

PCO Efficiency, Kinetics, and Reaction Quantum Yield

PCO performance was quantified by EtOH removal, the measure of the removal of the test VOC regardless of it being adsorbed or oxidized at pseudo-steady state conditions, and mineralization efficiency (X_A), the measure of complete oxidation of EtOH to CO_2. These values were calculated using Equations 1 and 2, respectively, where $[EtOH]_{IN}$ and $[EtOH]_{OUT}$ are the influent and effluent ethanol concentrations; $[CO_2]_{OUT}$ is the CO_2 generated by the PCO at pseudo-steady state conditions. The rate of the PCO of ethanol, r, was determined based on the formation of CO_2 rather than the disappearance of ethanol to prevent overestimation due to the

EtOH adsorption to the silica-rich photocatalyst. The reaction quantum yield (ξ), or photonic efficiency, was calculated as the ratio of the photocatalytic oxidation rate, r, to the incident photon flux, φ, as shown in Equation 3[8].

$$EtOH\ Removal = \left(\frac{([EtOH]_{IN} - [EtOH]_{OUT})}{[CO_2]_{OUT}}\right) * 100 \quad (1)$$

$$X_A = \left(\frac{[CO_2]_{OUT}}{2*[EtOH]_{IN}}\right) * 100 \quad (2)$$

$$\xi = \frac{r}{\varphi} \quad (3)$$

CHAPTER THREE: THE EFFECT OF PHOTON SOURCE ON THE PCO OF ETHANOL USING STCS

Spectral Quality of the UV-A BLB and UV-C GL

The Philips brand UV-A BLB was selected as the UV-A source because it was found to possess the highest light intensity over alternate UV-A fluorescent lamps previously tested[15]. The irradiance spectrum of the UV-A lamp (Figure 6A) had a broad primary peak (354-388 nm) centered at 365 nm and an additional peak at 405 nm that is beyond the band gap spectrum of anatase TiO_2 (λ<388 nm). The UV-C GL irradiance spectrum contained a high-intensity, narrow peak (250-255 nm) centered at 253 nm along with several low-intensity peaks at 313, 365, and 405 nm (Figure 6B)[8].

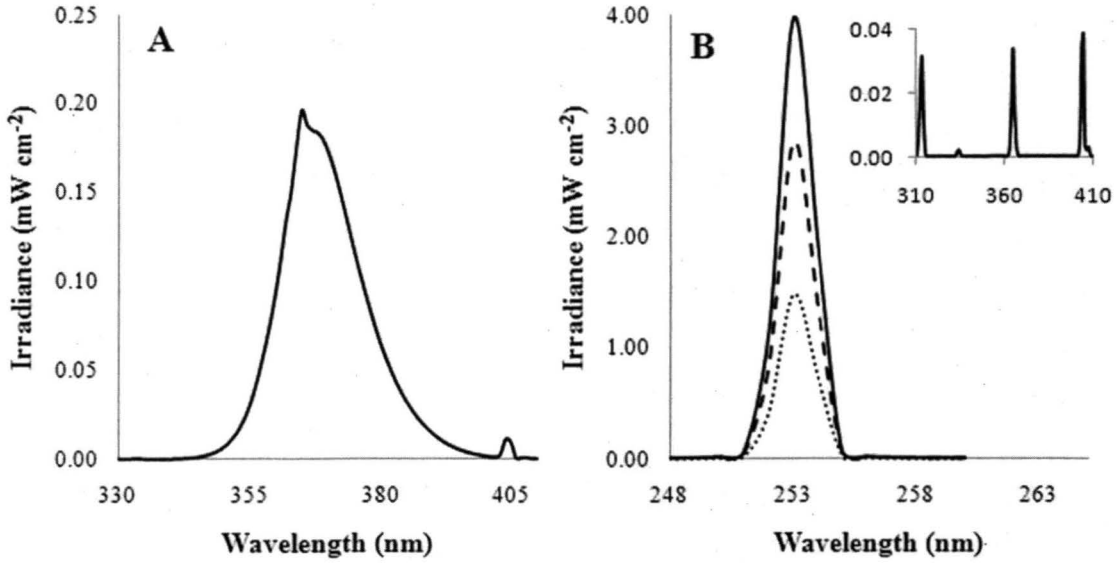

Figure 6: Average irradiance distribution for the (A) UV-A BLB at maximum irradiance and (B) UV-C GL at its maximum irradiance (solid line), attenuated irradiance using one layer of mesh

(dashed line), and attenuated irradiance using two layers of mesh (dotted line). The inset shows the secondary irradiance peaks for the full irradiance UV-C GL[8].

The irradiance of the primary peak for each lamp was determined through the integration of the irradiation scan with defined integration limits of 1% irradiance with respect to the value at the λ_{max}. The minor peaks for both sources were also integrated in a similar fashion to determine their contribution to the total irradiance of the lamps. It was found that the 405-nm peak accounted for 0.71% of the total irradiance of the UV-A lamp; the irradiances for the 313-, 365-, and 405-nm peaks in the UV-C source were found to account for 0.42%, 0.89%, and 1.06% of the total irradiance, respectively. Based on these results, it is not expected that these peaks had any significant contribution to the energy used in the activation of the TiO_2-assisted photocatalysis or possible photolysis of ethanol throughout this study. The irradiance at the surface of the catalyst, as well as the photon flux for both the UV-A source and UV-C source (with and without the neutral density filter), are shown in Table 1 (the values in Table 1 are the average of three scans with standard deviation; the photon flux is calculated to reflect that reaching the surface of the catalyst). The 8-W UV-C lamp had an irradiance 2.0 times higher than the 8-W UV-A source and was attenuated to obtain a range of intensities by the use of one or two layers of attenuation mesh[8].

Table 1: Average irradiance and photon flux for selected light sources.

Light Source	Irradiance ($mW\ cm^{-2}$)	Photon Flux ($\mu mol\ photons\ s^{-1}$)
UV-A BLB	3.49 ± 0.07	0.633 ± 0.013
UV-C GL + 2X Mesh	2.71 ± 0.07	0.337 ± 0.009
UV-C GL + 1X Mesh	5.17 ± 0.07	0.643 ± 0.009
UV-C GL + No Mesh	7.17 ± 0.07	0.892 ± 0.009

The Effect of Photon Flux of UV-C irradiation on STC-Catalyzed Oxidation of Ethanol

Figure 7 shows the change in carbon-normalized effluent composition over time after the introduction of contaminant flow and UV-C illumination. There were three compounds detected in the effluent stream: ethanol; CO_2, the complete mineralization product; and acetaldehyde (ACD), the only quantifiable intermediate detected by the GC-FID. A carbon balance for the system further confirmed this observation. For the UV-C source under all three intensities tested, the total carbon in the effluent and adsorbed onto the STCs accounted for a minimum of 94% of carbon entering the system (data not shown), which is within the range of error associated with the system[8].

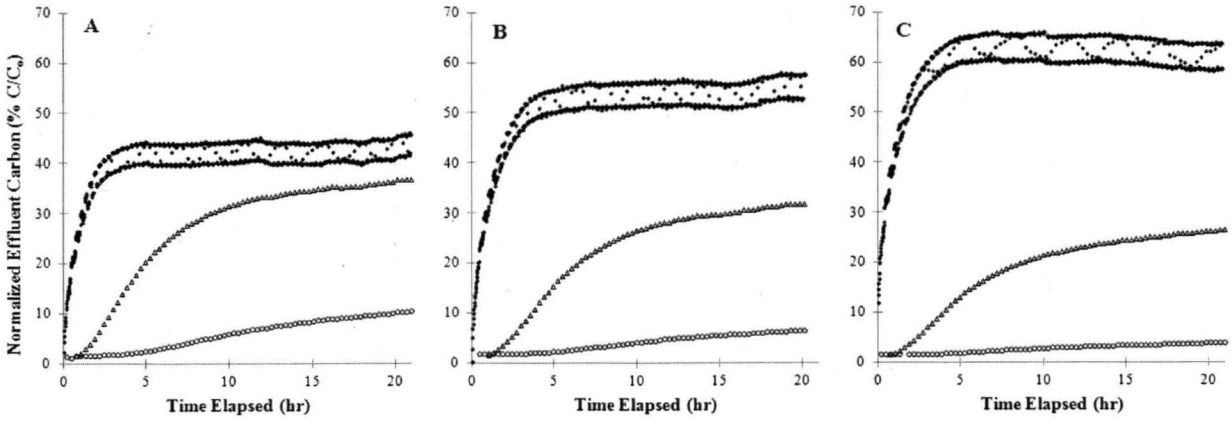

Figure 7: Time course of effluent composition (carbon-normalized) during STC-catalyzed oxidation of ethanol using the (A) UV-C GL with two layers of attenuation mesh, (B) UV-C GL with one layer of attenuation mesh, and (C) full-irradiance UV-C GL. Effluent species are designated as follows: (♦) CO_2 carbon, (Δ) ACD carbon, and (○) EtOH carbon[8].

The photon flux at the catalyst surface had a profound effect on the rate of effluent concentration increase and effluent composition at any given time point (Figure 7). A true

steady state was not attainable under the time restrictions of the experiments; thus, the pseudo-steady state, or time at which CO_2 formation reached a steady state and the change in effluent ethanol and ACD had reached a minimum, was implemented. The pseudo-steady state was achieved approximately after the ten-hour mark in all experiments. The average concentration between 10 and 20 hours was used to calculate the ethanol removal and mineralization efficiency. The concentration of components in the effluent stream is dependent upon the balance between their production and adsorption affinity to the STC pellets. The time it took for the initial appearance of each component in the effluent as well as the time to 50% of respective concentration at pseudo-steady state are good indicators for their affinity to STC pellets. CO_2 reached its 50%-concentration mark in less than 45 minutes for all experiments after the initiation of the EtOH-contaminated air flow; this suggests minimal, if any, adsorption of CO_2 to the STC pellets. In the cases of ACD and EtOH, this mark was attained within 5 hours and 8.5 hours, respectively. These results show lower adsorption affinity for ACD than for EtOH. Because of the low affinity for CO_2, its rate of evolution was used to determine the PCO rate. The PCO rate by STC-assisted photocatalysis was determined to be zero-order, regardless of the UV-C irradiance level implemented with respect to CO_2 evolution[8].

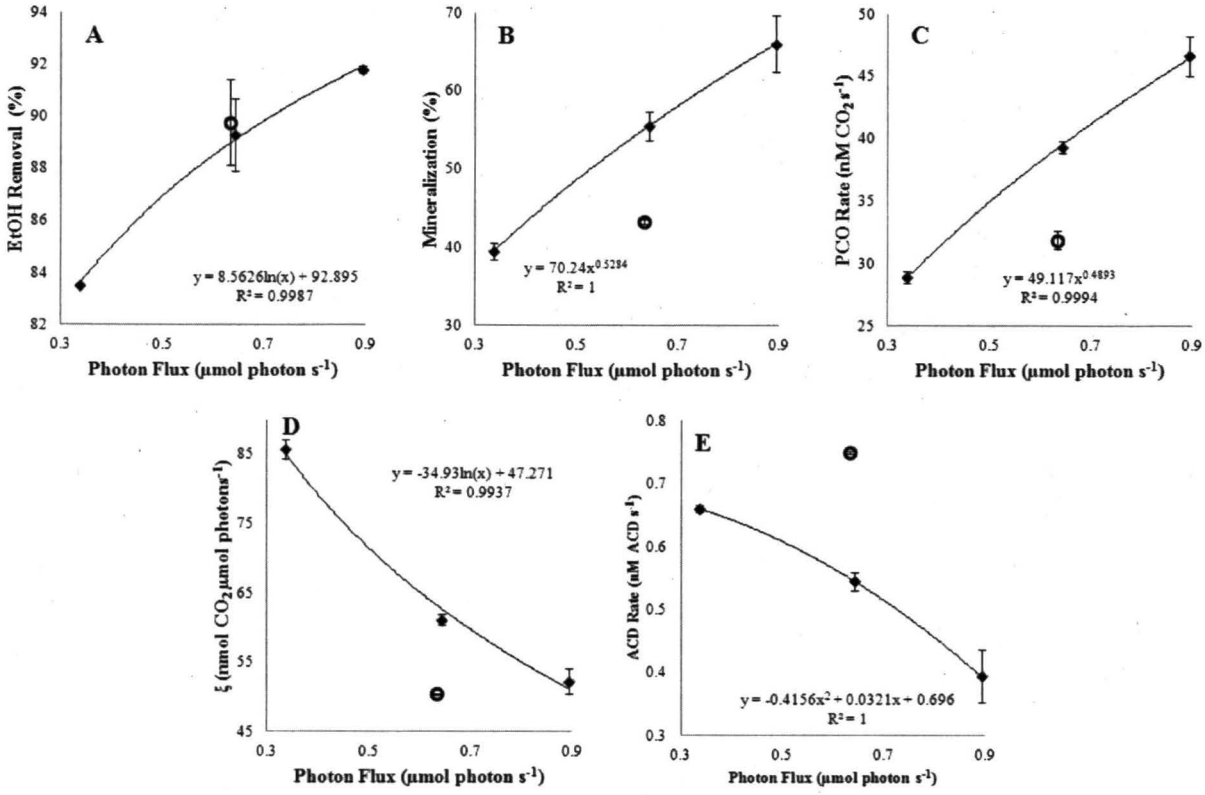

Figure 8: Relationships between photon flux and (A) ethanol removal (%), (B) mineralization efficiency (%), (C) PCO rate constant (nM CO_2 s^{-1}), (D) photonic efficiency, ξ, (nmol CO_2 µmol photons^{-1}), and (E) ACD evolution rate in the effluent (nM ACD s^{-1}). Data points designated with (○) were obtained using the UV-A light source and those designated with (♦) were obtained using the UV-C light source[8].

In general, increasing the photon flux at the catalyst surface resulted in an increase in ethanol removal (Figure 8A), ethanol mineralization (Figure 8B), and PCO Rate (Figure 8C). However, the reaction quantum efficiency decreased with the increase of photon flux (Figure 8D). The relationship between the photon flux (φ) and PCO rate (r) followed an exponential trend ($r=49.117\ \varphi^{0.489}$) over the range of intensities studied. Previous reports by Egerton and King[45] proposed that the dependence of the PCO reaction rate on the photon flux follows a

first-order kinetic trend ($r=K\varphi$, where K is a constant) when φ is 0.008 μmol photons s^{-1} or lower, but follows a half-order kinetic trend ($r=K\varphi^{0.5}$) when φ exceeds this photon flux[45]. Since the photon flux employed in this study was in the range of 0.337-0.892 μmol photons s^{-1}, our results are in close agreement with the relationship proposed by Egerton and King[45]. There were several differences between our system and that used by Egerton and King[45] including 1) the use of the Degussa P25 TiO_2 opposed to the 100% rutile TiO_2 used by Egerton and King[45] where the crystal structure may have played a role in the kinetics differently; 2) the use of a UV-C light source, and thusly, higher-energy photons (only UV-A light sources were tested previously); and 3) the use of the STC instead of a TiO_2 thin film: the former is not only much thicker (5 mm) than the latter, it also contains less TiO_2 for the same surface area exposed to the light (Figure 3). Regardless of these changes, the same relationship was developed. Furthermore, our results indicate that the relationship developed between photon flux and PCO rate by Egerton and King[45] is independent of wavelength[8].

As a result of the decreased dependency of the PCO rate on photon flux within the range tested, the reaction quantum efficiency decreased as the photon flux increased (Figure 8D). This result implies that not all of the charge carriers generated in this range of photon flux were utilized in the redox process; furthermore, less reactive carriers may have accumulated and undergone recombination. In other words, energy-use efficiency decreases at a significantly large photon flux even though it leads to increased mineralization (Figure 8B) and reduced intermediate evolution (Figure 8E). A balance between energy-use efficiency and PCO efficiency must be scrutinized in the design of such PCO reactors[8].

As mentioned, the PCO of ethanol on a TiO_2 surface is known to follow several similar pathways that can include various intermediates such as acetaldehyde, acetic acid, formaldehyde, and formic acid[20]. While acetaldehyde was the only intermediate detected in our system, this does not mean that acetic acid, formic acid, and formaldehyde did not form during our reaction but suggests that they were oxidized at the same (or faster) rate they were formed. Therefore, a simplified mechanism of the reaction (Figure 9) was used to better understand the decreased evolution of acetaldehyde with increased photon flux (Figure 8E)[8].

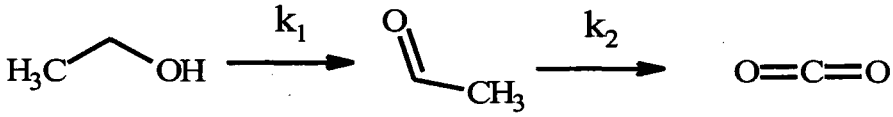

Figure 9: Simplified reaction for the photocatalytic degradation of ethanol

The fact that there was a significant amount of ACD in the effluent suggests that k_2 is slower than k_1; i.e., the oxidation of acetaldehyde is the rate-limiting step in the mineralization of ethanol. Furthermore, it may be assumed that the adsorption of ACD onto the STCs is not affected by photon flux since the time at which the 50% pseudo-steady state concentration mark was reached was equivalent for all light intensities studied. Although both the oxidation of ethanol to acetaldehyde (k_1) and that of acetaldehyde to CO_2 (k_2), was accelerated by increased light intensity, the evolution of ACD in the effluent decreased as the photon flux increased. This implies a greater increase in k_2 than k_1. Therefore, this result suggests that it is possible to eliminate the accumulation of ACD if sufficient light intensity and optimized reactor design are provided[8].

The Effect of Wavelength (UV-A vs. UV-C irradiation) at the Same Photon Flux

The PCO of ethanol by STCs irradiated by a UV-A light source was investigated under the same conditions and in the same reactor as that used in the former UV-C experiments. The key performance parameters including ethanol removal, mineralization efficiency, PCO rate, photonic efficiency, and ACD evolution are summarized in Table 2 (values were given with standard deviation, where appropriate). The corresponding performance data for a reactor illuminated with UV-C light at the equivalent photon flux of the UV-A source (i.e., 0.633 ± 0.013 μmol photons s^{-1}) was extrapolated from the relationships obtained in Figure 7 to allow for a direct comparison[8].

Table 2: Effect of photon energy on PCO Performance

Light Source	EtOH Removal (%)	Mineralization (%)	PCO Rate (nM CO_2 s^{-1})	ξ (nmol CO_2 μmol photons)	ACD Rate (nM ACD s^{-1})
UV-A BLB	89.8 ± 1.6	43.4 ± 0.3	31.9 ± 0.7	50.5 ± 0.1	0.750 ± 0.002
UV-C GL[c]	89.0	55.1	39.3	63.3	0.549

As seen in the UV-C studies, ACD was also the only quantifiable intermediate in the UV-A studies; however, ACD evolution was much higher than seen in any of the UV-C experiments. The total carbon balance for the UV-A-irradiated system was 94.6% again confirming the claim that was no accumulation of other intermediates. The EtOH removal for the UV-A-illuminated reactor (89.8 ± 1.6%) was statistically equivalent to the projected EtOH removal (89.0%) for the UV-C-illuminated reactor at the equivalent irradiance. However, this equivalence is not due to equivalent mineralization and PCO rate (Table 2), but is likely attributed to an accelerated k_1 and

reduced k_2, that is, an increased oxidation of ethanol to acetaldehyde and reduced oxidation of acetaldehyde to CO_2, allowing for increased evolution of ACD in the UV-A-irradiated reactor[8].

Similar to the results from the UV-C illuminated experiments, it was found that the rate of evolution of CO_2 followed a zero-order rate law when the UV-A photon source was used. The PCO rate at the equivalent photon flux was 31.9 ± 0.7 and 39.3 nM CO_2 s^{-1} for the UV-A BLB and UV-C GL, respectively. This demonstrated that photons with a shorter wavelength (or higher energy) increase the PCO rate ($r_{UV\text{-}C} > r_{UV\text{-}A}$). Moreover, the reaction quantum efficiency for an equivalent-photon flux UV-C-illuminated reactor was 1.25 times that of the UV-A-illuminated reactor; this is consistent with the previous findings that shorter wavelength photons render greater chemical quantum yield in crystalline TiO_2 sols or metastable TiO_2[26], although the magnitude of the enhancement is dependent on the catalyst used. According to Grela et al.[46], chemical quantum yield increases significantly with an increase of excess photon energy, E_λ, over the bandgap energy, E_{bg}, according to $E^* = E_\lambda - E_{bg}$ and reaches a plateau at $E^* = \sim 0.9$ eV. In this study, the UV-A BLB gives an $E^* = 0.2$ eV while the UV-C GL gives $E^* = 1.7$ eV over the anatase TiO_2 bandgap of 3.2 eV. Our results support the theory and predict that UV-B (290 – 320 nm) range irradiance would give rise to the same efficiency as UV-C[8].

These results suggest that a shorter wavelength light source, or photons of higher energy, has an overall positive effect on the PCO of ethanol. Taking into consideration that only ~10% of UV-C light (compared to ~90% of UV-A light) is transmitted through a single layer of TiO_2 thin film[22], less catalyst surface was directly exposed to the UV-C photons. The enhanced performance of the shorter wavelength source is more likely to be the result of 1) increased formation of potential active species in the photocatalytic oxidation reaction[47], 2) reduced

electron-hole recombination[26], 3) increased interfacial electron transfer between TiO_2 particles, and/or 4) increased probability for direct photo-oxidation of ethanol. This last hypothesis was tested by packing the reactor with 3-mm glass beads instead of STC pellets and examining whether ethanol was degraded by UV light alone[8].

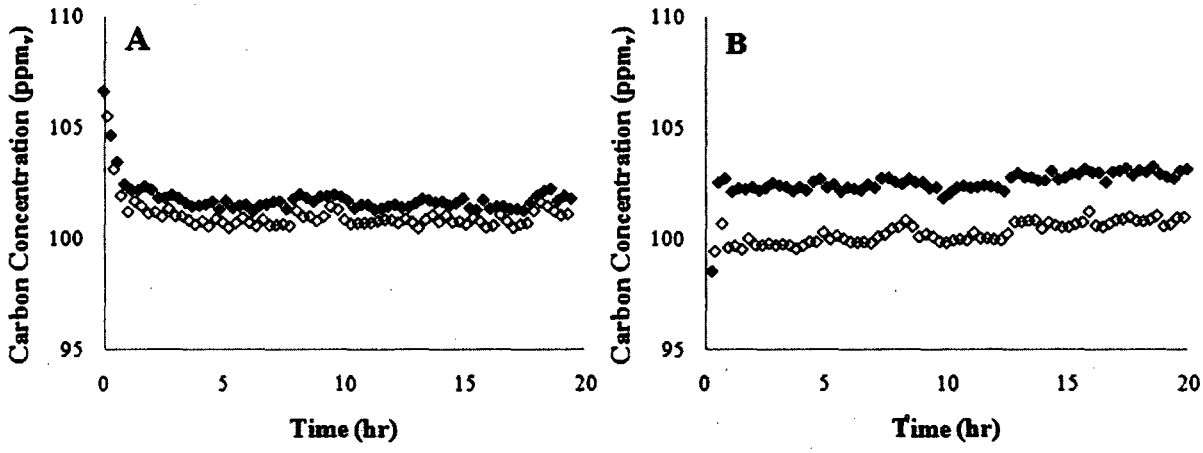

Figure 10: Influent (♦) and effluent (◊) EtOH composition during photolysis of ethanol by the (A) UV-A BLB and (B) UV-C GL light sources[8].

No significant difference in EtOH concentration between the influent and effluent was found during the experiment utilizing the UV-A BLB (Figure 10A). Furthermore, no CO_2 or ACD above the baseline level was observed in the effluent under UV-A illumination. Conversely, in the UV-C-irradiated reactor, a small quantity of ACD (average 1.36 ppm_v ACD) was found in the effluent, accompanied by a small decrease in EtOH concentration between the influent to the effluent (Figure 10B). Clearly, differential photooxidation by UV-C and UV-A plays a small role in ethanol mineralization and is not the main contributing mechanism for the

11.7% higher mineralization efficiency, 7.4% increased PCO rate, and more 1.25 times higher reaction quantum efficiency seen in the UV-C PCO reactor over that in the UV-A reactor[8].

CHAPTER FOUR: ADSORPTION-ASSISTED PCO DEPENDENCE ON TEMPERATURE AND RELATIVE HUMIDITY

Temperature Effects on the PCO and STC-Adsorption of Ethanol

STC Adsorption Capacity and Temperature

Similar to Fu et al[28], no appreciable ethanol oxidation was seen in the absence of UV irradiation at any of the temperatures studied, verifying that no thermal catalytic oxidation occurred. These dark temperature experiments also gave rise to trends in ethanol adsorption on the STC catalyst; with an increase from 25°C to 35°C, there was a 17.8% increase in ethanol adsorption to the catalyst (Figure 11). Increasing the temperature further, however, led to a significant decrease in ethanol adsorption capacity of the STCs.

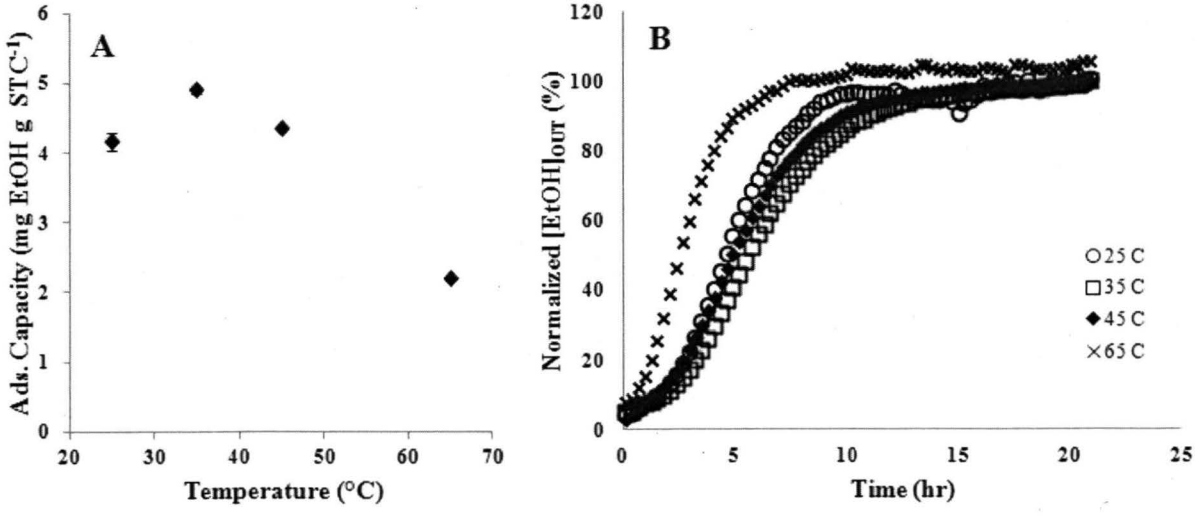

Figure 11: (A) Changes in ethanol adsorption capacity of STCs with temperature and (B) changes in ethanol breakthrough with temperature.

Fu et al[28] described an increase in PCO activity for the degradation of ethylene with increased temperature due to the dramatic desorption of water from the catalyst surface, explaining the increased adsorption of ethanol at 35°C. At the higher temperatures, it is apparent that ethanol is also being driven off of the catalyst causing a decrease in adsorption capacity. Figure 11B shows the relationship of $[EtOH]_{OUT}$ over time with respect to temperature. Adsorption breakthrough curves for 25-45°C share similar shape and are close in the 95% breakthrough point for ethanol (~12.5 hours). A 50% decrease in the 95% breakthrough curve was observed when the temperature was raised to 65°C, correlating with the decrease in ethanol adsorption.

Temperature Effect on PCO of Ethanol

Temperature is seen to play a positive and crucial role in the efficiency of STC-assisted photocatalytic oxidation of ethanol. Figure 12 clearly shows that moderately increasing the temperature significantly enhanced the mineralization efficiency (Figure 12B), PCO rate (Figure 12C), and reaction quantum efficiency (Figure 12D), while the ethanol removal did not change greatly (Figure 12A). As a result of increases in mineralization/PCO rate and no great increase in ethanol removal, the acetaldehyde evolution rate also decreased by approximately 50% when the temperature was increased to 65°C from 25°C (Figure 12E). With lower adsorption of VOCs at higher temperatures, reduction of acetaldehyde formation is expected with an enhanced selectivity of the complete oxidation product, CO_2, as seen by the increase in mineralization efficiency due to little change in total ethanol removal (Figure 12A). Referring to the simplified reaction scheme based on our reaction intermediates and products (Figure 9), this would indicate a greater increase in k_2 over that of k_1 leading to less buildup of acetaldehyde in the reactor

effluent. Comparable to the photon source, no other intermediates were detected in the reactor effluent.

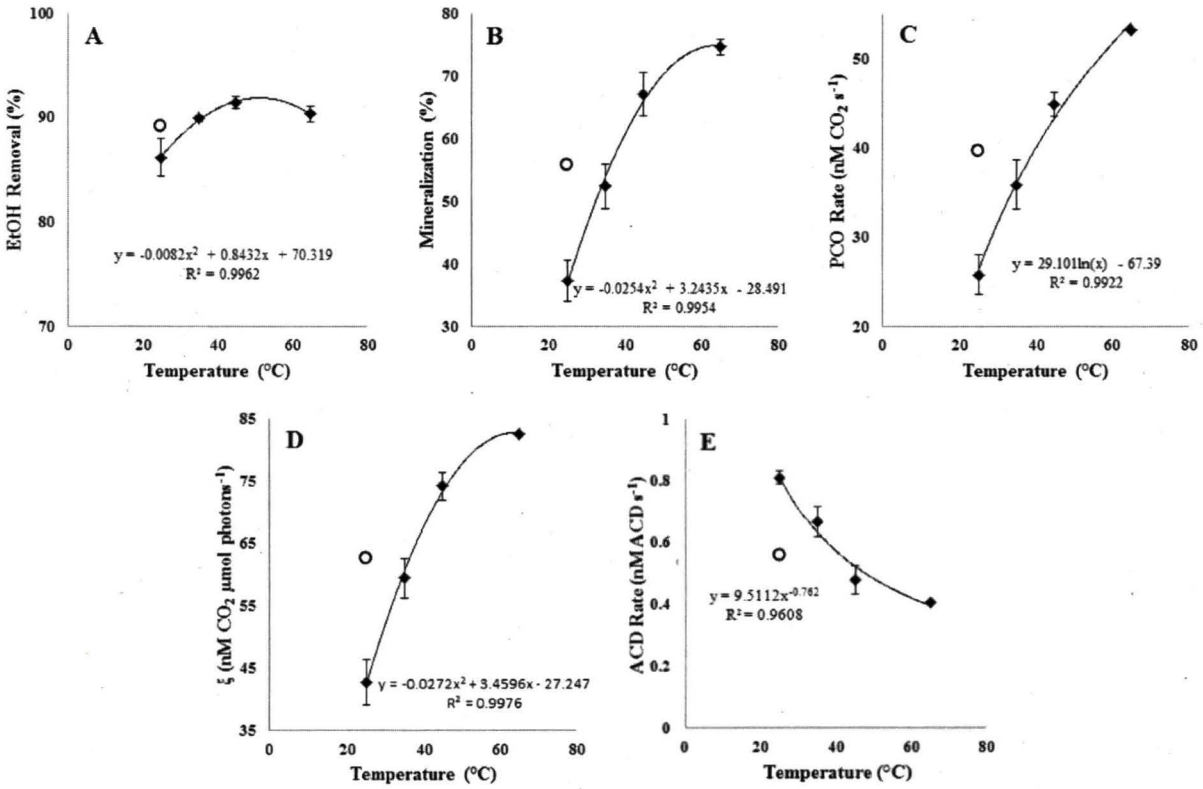

Figure 12: Relationships between temperature and (A) ethanol removal (%), (B) mineralization efficiency (%), (C) PCO rate constant (nM CO2 s^{-1}), (D) photonic efficiency, ξ, (nmol CO2 µmol photons-1), and (E) ACD evolution rate (nM ACD s^{-1}). Data points designated with (♦) were obtained using the UV-A light source and those designated with (○) were extrapolated from the relationships in Figure 8 for a UV-C with the same photon flux as the UV-A light source used in the temperature series studies.

Over the range of temperatures assessed, the mineralization efficiency, PCO rate, and reaction quantum efficiency were not seen decrease, but may have reached a maximum as indicated by their parabolic trends; further temperature profiling must be completed to determine

if these are indeed maximum values or if a plateau is occurring. This trend of reaching a maximum reaction rate followed by a considerable decrease was explained by Westrich et al[32] with the indication that, with higher temperatures, the contribution of UV photons diminishes due to a possible loss of photo-generated charge carriers. The loss of these charge carriers can take place via multiple routes including radiative recombination (temperature independent), nonradiative recombination (temperature dependent), and charge transfer to intermediate species with the final result being product formation[32]. In nonradiative recombination, inelastic collisions between charge carriers and phonons result in lost charge carrier energy and occur with increasing probability as temperature increases due to the increase in number of high-energy phonons and in phonon-phonon interaction rates[32]. This type of recombination is becomes most significant at temperatures equal to or greater than 247°C for rutile and 327°C for anatase TiO_2[32]. It is not likely that nonradiative recombination is playing a major role in charge carrier loss in the current studies, as the reactor was not operated at these extremes.

Use of Elevated Temperature and UV-A Light as an Alternative to UV-C Light

As discussed in Chapter 1, Fu et al[28] argues that energy utilization in the majority of photocatalytic systems is inefficient because most reactors are operated at room temperature by cooling the apparatus rather than utilizing the heat evolved from the light source to enhance PCO activity. Similarly to the light source characterized for output efficiency by Fu et al[28], the UV-A light source implemented in the current studies utilizes only 17.5% of the electrical energy input to produce UV light, while the remaining electrical energy is transformed into heat. The UV-C light source utilized in the current studies is much more efficient utilizing 31% of the electrical energy for production of UV light. While it was demonstrated that UV-C photons were

1.25 times more efficient than UV-A photons for the PCO of ethanol at the same photon flux[8], moderately elevating the temperature of the PCO reactor allows for skyrocketing efficiency of UV-A light sources over that of UV-C light sources (Figure 12). A rise of 10°C allowed for near equivalent performance of UV-A photons for EtOH removal (Figure 12A), mineralization (Figure 12B), PCO Rate (Figure 12C), and reaction quantum efficiency (Figure 12D). This rise in temperature also decreased the ACD evolution in the effluent stream, however ACD evolution with UV-C irradiation at room temperature was still slightly lower (0.671 nM ACD s^{-1} vs. 0.563 nM ACD s^{-1} for UV-A and UV-C irradiation, respectively). Without external cooling, the temperature of the PCO reactor system was found to be approximately 45°C when using the UV-A light source. At this temperature there is a 34.2% increase in mineralization efficiency, 34.3% increase in PCO rate, and 31.8% increase in reaction quantum efficiency for UV-A photons over UV-C photons at room temperature. Slight elevation of temperature can be used to better design a UV-A LED-based reactor (since UV-C LED technology has not yet reached practical efficiency for application) with minimal electrical energy additions to create a system that can achieve high efficiency without the hazards associated with traditional fluorescent lamps.

Relative Humidity Effects on the PCO and STC-Adsorption of Ethanol

STC Adsorption Capacity and Relative Humidity

With an increase in relative humidity, there was a significant decrease in ethanol adsorption capacity as seen in Figure 13A. The higher the relative humidity, the lower the initial $[EtOH]_{OUT}$ and the faster breakthrough occurred (as denoted by the steeper slope of the adsorption curve). The time for 95% breakthrough to occur was 48.5, 28.1, and 16.8 hours for

17%, 45%, and 75% RH, respectively. The decrease in adsorption capacity with increasing RH signifies the competitive adsorption between water and ethanol molecules on the catalyst as described by multiple other studies[28, 33, 35, 36]. Stokke and Mazyck[48] studied the adsorption of methanol on the STCs at 12% and 95% RH finding 11 mg MeOH g $STCs^{-1}$ (0.3433 mmol MeOH g $STCs^{-1}$) and 1.2 mg MeOH g $STCs^{-1}$ (0.0375 mmol MeOH g $STCs^{-1}$) adsorption capacities, respectively. If the adsorption capacity for ethanol at the same RH values is extrapolated from the linear relationship in Figure 13A, the values would be 17.6182 mg EtOH g $STCs^{-1}$ (0.3824 mmol EtOH g $STCs^{-1}$) at 12% RH and 2.1055 mg EtOH g $STCs^{-1}$ (0.0457 mmol EtOH g $STCs^{-1}$) at 95% RH. These values are in close agreement with the molar amounts determined by Stokke and Mazyck[48] and show molar adsorption capacity for similarly polar compounds on the STC pellets.

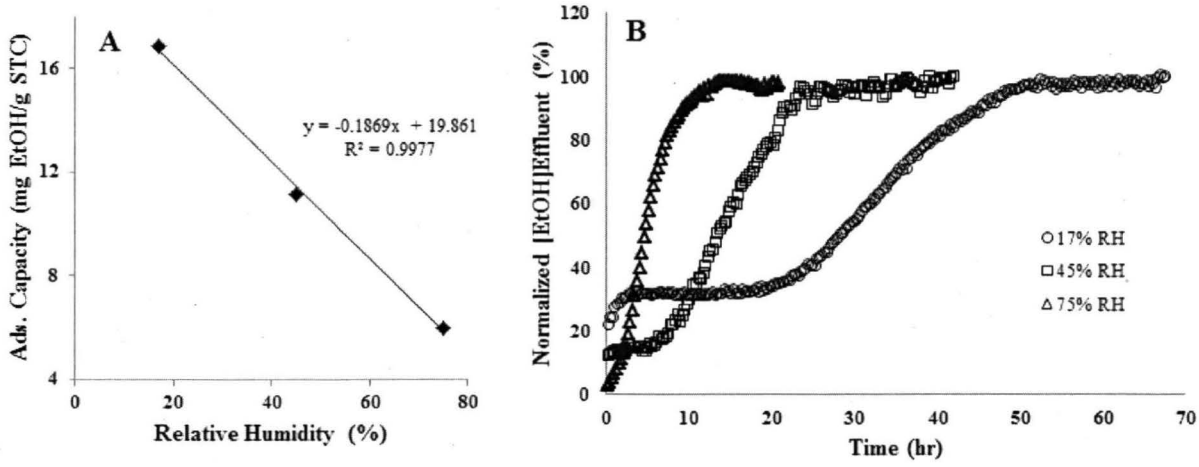

Figure 13: (A) Changes in ethanol adsorption capacity of STCs with relative humidity and (B) changes in ethanol breakthrough with relative humidity.

Humidity Effects on the PCO of Ethanol

Over the range of 17% to 75% RH, there were obvious relationships in the parameters examined; however, these correlations were not as influencing as those seen with alterations in temperature.

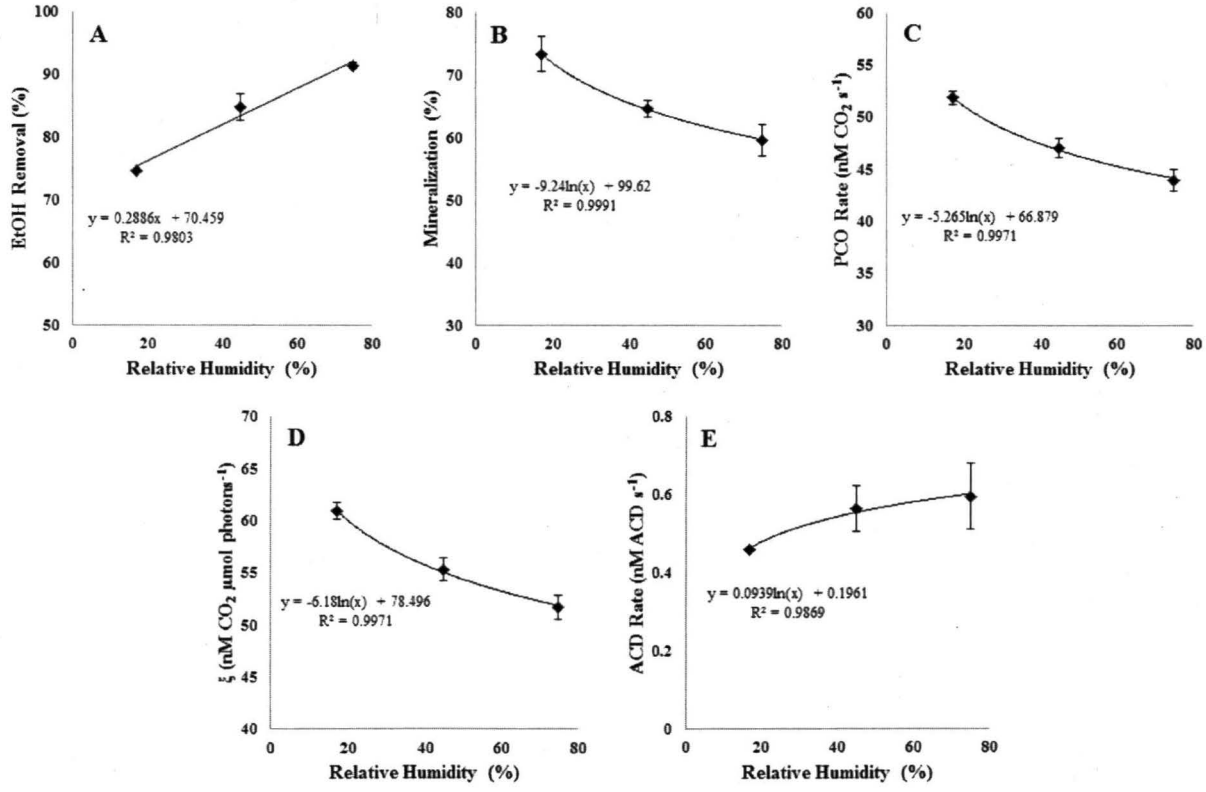

Figure 14: Relationships between relative humidity and (A) ethanol removal (%), (B) mineralization efficiency (%), (C) PCO rate constant (nM CO_2 s^{-1}), (D) photonic efficiency, ξ, (nmol CO_2 µmol photons^{-1}), and (E) ACD evolution rate in the effluent (nM ACD s^{-1}).

The most pronounced difference was increased ethanol removal with increased relative humidity (Figure 14A). This increase was not due to increased EtOH adsorption as depicted in

Figure 13A and is also not due to increased mineralization (which was seen to decrease with increasing RH in Figure 14B). Increased RH can lead to heightened concentrations of hydroxyl radicals on the catalyst surface resulting in high reaction rates[35], though a decrease in both mineralization and PCO rate was seen to occur. As discussed by Muggli et al[20], water molecules play a role in which degradation pathway is pursued during EtOH photocatalytic oxidation; there was a slight increase in ACD evolution rate (Figure 14E), which explains the increase in EtOH removal and decrease in mineralization efficiency. Besides the competitive adsorption of EtOH and water at higher RH values, there is likely also competition at the specific sites that allow for subsequent oxidation of ACD to CO_2, showing adsorption preference of water, followed by ethanol, followed by ACD.

Mineralization efficiency, PCO rate, and photonic efficiency were all seen to have a negative correlation with increasing relative humidity (Figure 14B, C, and D). These findings correlate with humidity studies on the photocatalytic oxidation of ethylene[28], and TCE[24, 35], and are opposite to the findings of the dependence of toluene oxidation and increasing humidity[33, 34]. The data from the current studies further implies the effect of RH on photocatalytic oxidation greatly depends on the target VOC, the competitive adsorption of the VOC and water on the catalyst, and the role of water in the possible degradation mechanism of the VOC. While the trends for these parameters as seen in Figure 14 are all negative, the slope and possible plateau effect of the trends show that relative humidity does not cause dramatic changes in the PCO performance as is seen for temperature (Figure 12) and photon flux (Figure 8).

CHAPTER FIVE: STC POISONING STUDIES

Low-Level VOC Room Air Challenge

In order to accurately assess the estimated lifetime of the STC catalyst, exposure of the STCs to laboratory air simulated the low-VOC environment of a closed habitat system. Polar organic compounds present in the laboratory air were assessed by bubbling laboratory air through a set of glass impingers containing e-pure water. The resulting solutions were analyzed on a TOC analyzer. An average of 1.44 ± 0.19 ppm TOC was calculated for a 24-hour period. While this represents an estimate of polar organic compounds, it does not account for nonpolar organic compounds that are less soluble in water nor any inorganic gases introduced to the reactor system.

A qualitative profile of trace contaminants found in the laboratory air was also completed using SPME technology. The SPME fiber was exposed to laboratory air for a 45-hour period and subsequently processed using GC-MS. Figure 15 shows the chromatogram and identity of the various compounds detected from the SPME study. Of the compounds identified, several (i.e., touene, 2-butanone, xylenes) are directly used and/or stored in the laboratory, many are compounds utilized in perfumes or other scented toiletries (i.e., hexanal, octanal, methyl heptanone, nonanal, decanal, tetradecane, benzophenone), and others are commonly found as compounds from instrumentation/equipment offgassing from plactisizers, rubbers, protective coatings, etc. (i.e., methyl isobutyl ketone, aniline, styrene, tetradecane, pentadecane. 2-ethyl-1-hexanol, benzothiazole).

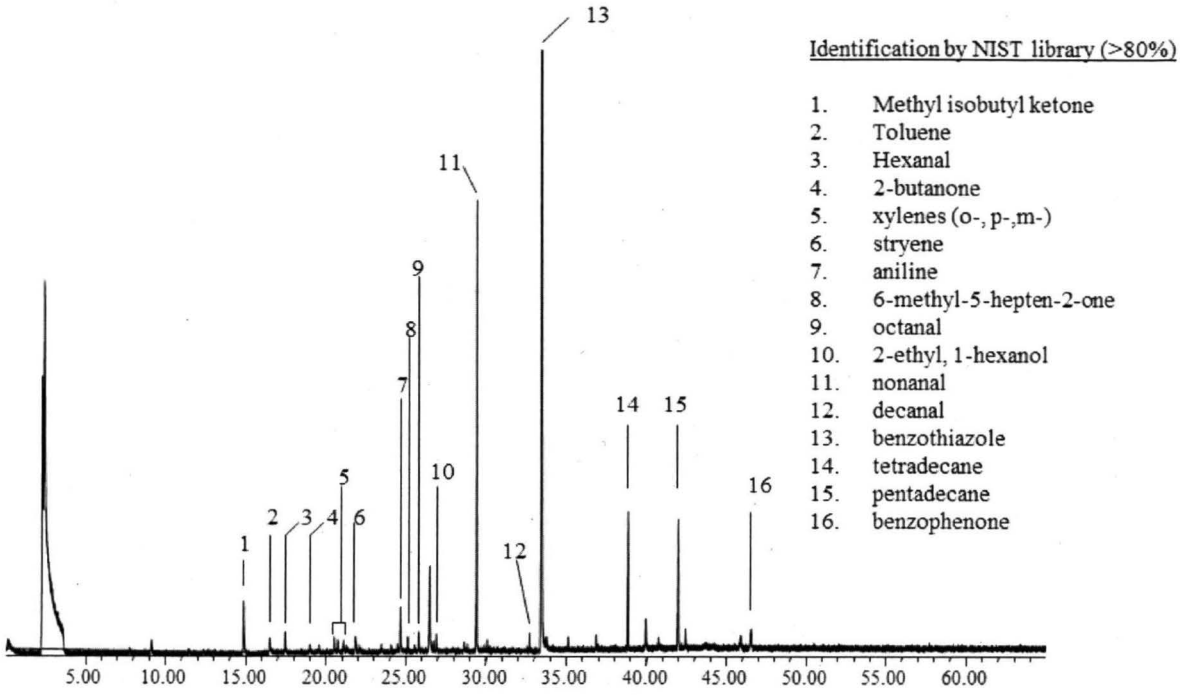

Figure 15: Chromatogram of SPME analysis of laboratory room air after 45 hours of exposure.

To date, the low-VOC study has been assessed over an eight-week period, with continuing time points still in progress. As seen in Figure 16A, the ethanol removal has remained relatively constant over the time course of the study; the PCO rate (Figure 16B) decreased by 6.4% after two weeks of exposure followed by a further 4.9% after six weeks of exposure. At the eight-week check, the PCO rate had regained ~3.2% activity; the drop at the week six checkpoint may have been due to not fully-regenerating the STC bed with VOC-free sweeping gas and UV illumination prior to testing. Since the PCO rate is obtained by the evolution of CO_2 in the system, signifies that the mineralization efficiency of the catalyst (and thus, the reaction quantum efficiency) also decreased after the two-week exposure; both have

remained nearly constant between the two-week and eight-week checkpoints. Since the EtOH removal capacity of the STCs did not change and a decreased mineralization capacity was found, the amount of acetaldehyde (the only intermediate detected) evolved should be seen to increase as is shown in Figure 16C; this value, however, has not deviated drastically throughout the study.

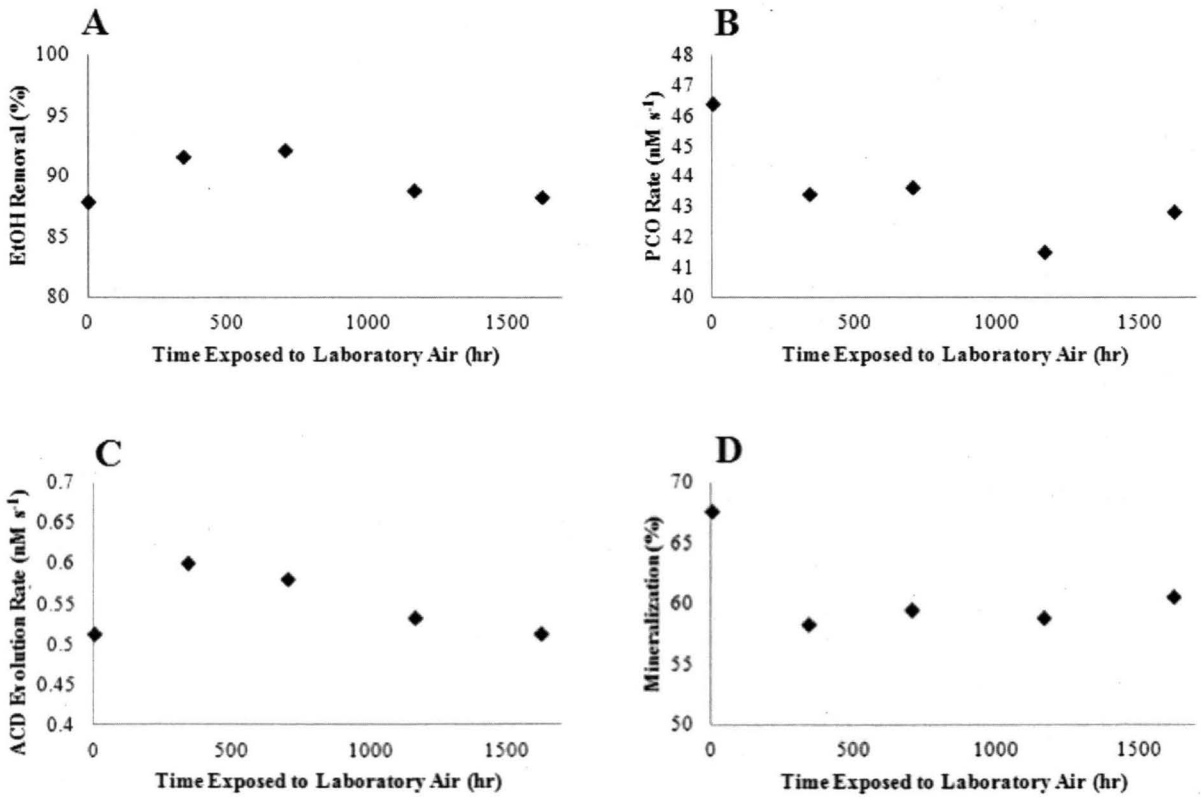

Figure 16: Effect of low-VOC air on STC activity over extended operation time with respect to A) ethanol removal (%), B) photocatalytic oxidation rate (nM CO_2 s^{-1}), C) acetaldehyde evolution rate (nM ACD s^{-1}), and D) mineralization efficiency (%).

The slight decline in PCO activity could be due to the strong adsorption of various species over the adsorption of the test contaminant, ethanol. However, this seems unlikely as the overall ethanol removal has remained consistent over time. As With elevated acetaldehyde

evolution after two weeks of laboratory air exposure; it is likely that if competitive adsorption is occurring, it may be occurring at the active sites where acetaldehyde is strongly bound and subsequently oxidized. According the mechanism proposed by Muggli et al[20], ethanol is oxidized on at least two types of sites; on one site, the acetaldehyde desorbs readily, and on the other site, the acetaldehyde is strongly bound. Applying this theory to the current study, it would appear that any adsorption changes are occurring at the sites where acetaldehyde is further oxidized. While it has not been currently tested for the STC catalyst, heating the catalyst to drive off adsorbed species similarly to the method used by Muggli et al[20] may allow for sufficient regeneration to recover the loss in photocatalytic activity, though the loss is currently not drastic enough to warrant extreme measures.

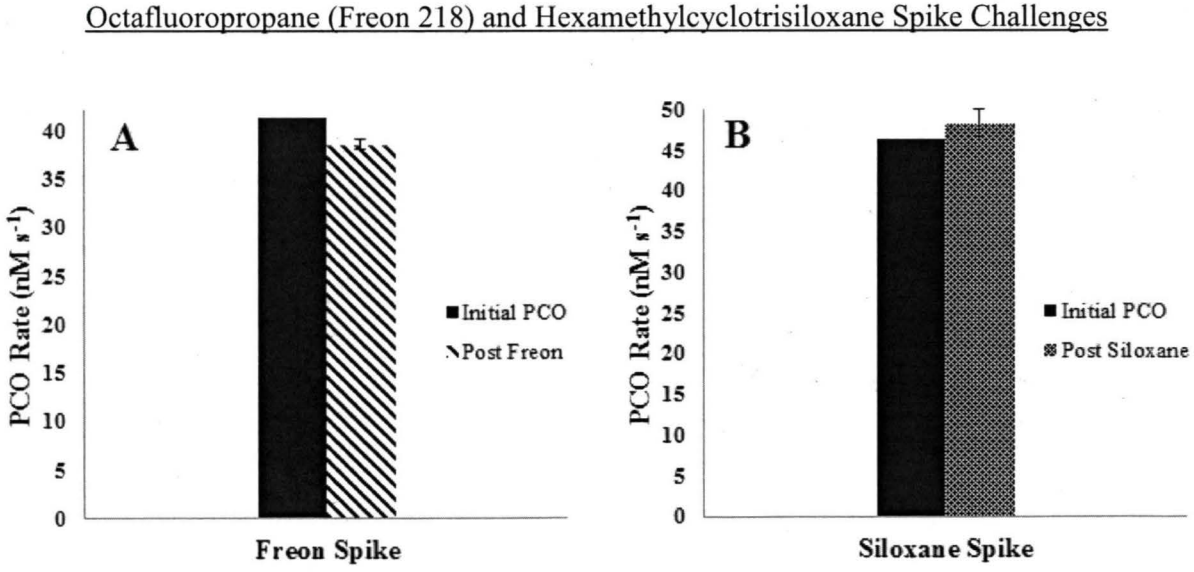

Figure 17: Changes in PCO rate after exposure to A) Freon 218 and B) hexamethylcyclotri-siloxane contaminants.

Akin to the results seen with the low-concentration VOC testing, the PCO rate was seen to decrease by 6.7% after a 24-hour exposure to 78 ppm_v Freon 218 at a 2 L/min flow rate through the reactor (Figure 17A); it was also seen that the total ethanol removal remained constant and that as a result, the ACD evolution rate increased. This concentration of Freon 218 was chosen as the spike level to represent an episodic leak of the compound equivalent to the concentrations previously detected on at least two occasions in the ISS cabin air[37]. Repeated exposure to this concentration of the Freon did not cause any further degradation in catalyst activity. Analysis of the effluent airstream during the Freon 218 poisoning study revealed that by five hours the Freon concentration was nearly equivalent to the influent concentration (Figure 18). No other intermediates were detected by GC-MS, leading to the conclusion that there was minute adsorption of the Freon to the catalyst. Further analysis of the catalyst via XPS (Table 3) found no differences in the catalyst surface; unlike Karmakar and Greene[41] and Farris et al[42] where catalyst surfaces were fluorinated by the Freon contaminant suffering irreversible deactivation.

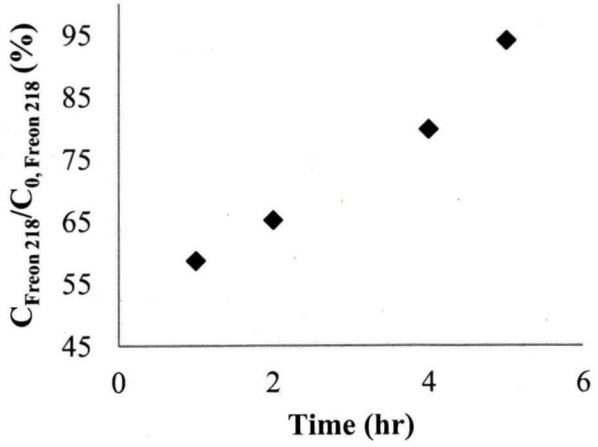

Figure 18: Freon 218 effluent concentration time course for Freon spike testing.

Table 3: XPS Binding Energy Peaks for STCs Pre- and Post-Exposure to Freon 218 and Hexamethylcyclotrisiloxane

Sample	O1s	Si2p	Ti2p
Pre-Exposure	532.90	103.35	458.32
Post-Freon 218	533.06	103.90	458.34
Post-Siloxane	532.95	103.47	458.49

Contrary to the other results seen[38, 39], it was determined that the initial PCO and post-siloxane exposure PCO rates are statistically equivalent (Figure 17B). This is substantiated by no significant change in acetaldehyde evolution rate or in ethanol removal capacity. Previously mentioned studies by Sun et al[39] and Hay et al[38] described the photocatalytic degradation of octamethyltrisiloxane and tetramethylsilane, respectively; both groups described the deactivation of TiO_2 due to the deposition of SiO_x groups on the catalyst surface (along with the evolution of CO_2 due to the mineralization of the methyl groups on the siloxane). Sun et al[39] used a high concentration of siloxane (25-45 ppm_v) while Hay et al[38] used a lower concentration (1 ppm_v) similar to the test concentration utilized in this study (0.247 ppm_v). This concentration was chosen to reflect the average overall siloxane concentration found in the ISS cabin air. No hexamethylcyclotrisiloxane, or other silicon-containing compounds were detected in the effluent stream of the reactor; the expected level of CO_2 evolved from the degradation of the siloxane is also below the limit of detection of the GC-FID and GC-MS instrumentation. These results led to two possibilities regarding the fate of the siloxane: 1) the siloxane was adsorbed to the catalyst surface and/or 2) the siloxane degraded completely and the silicon-containing products were adsorbed on the catalyst surface. SEM and XPS (Table 3) analyses did not show any differences in the catalyst surface post-siloxane exposure. Both Hay et al[38] and Sun et al[39] used thin-layer-coated catalyst surfaces when deactivation due to siloxane exposure was dramatic. The

STC pellets differ greatly from thin-layer coatings since they are not dependent on a single layer of catalyst but instead are highly porous; thus, regardless of the siloxane adsorbing or degrading and depositing SiO_x onto their surface, the concentrations in ISS cabin air are not enough to restrict all pores and active sites; a much larger amount (or much longer exposure time) would be required to cause noteworthy deactivation of the STC activity.

CHAPTER SIX: CONCLUSIONS

This study demonstrated that optimization of photocatlaytic systems requires meticulous detail to many parameters including the choice of light source, reactor temperature, and humidity level to achieve high mineralization efficiency combined with low intermediate evolution. Furthermore, a paramount assessment, as with any catalytic system, is the determination of possible deactivation events through mechanisms such as chemical poisoning as well as the overall lifetime of the system to ensure a safe environment in closed habitat systems.

Both photon flux and photon energy have profound impacts on not only the PCO efficiency, but also on the energy-use efficiency and must be scrupulously taken into consideration in the design of an efficient PCO reactor. As the photon flux increased for the UV-C source, the quantum yield decreased. In accordance with previous studies, the mineralization efficiency for ethanol and PCO reaction rate increased with the incident photon flux within the range examined. This study also demonstrated that 254-nm photons (UV-C) are 1.25 times more efficient than 365-nm photons (UV-A) at the same irradiation level for driving the STC-catalyzed degradation of ethanol in the gas phase. This is in agreement with the findings by Grela et al.[26] and Paz[47] for the oxidation of salicylate (3.8 to 6.4 times depending on substrate concentration) and 3-nitrophenol, respectively. The extent of photooxidation of ethanol in the absence of the STCs by higher energy photons (254 nm) was slightly higher than that of lower energy photons (365 nm), but not sufficient to contribute to the increase in photonic efficiency, PCO rate, and mineralization efficiency. It is concluded that the enhanced performance by shorter wavelength photons from the UV-C light source is due to the combined

result of increased active charge carriers, reduced electron-hole combination, and increased interfacial electron transfer between TiO_2 particles.

The effect of temperature and relative humidity on the STC-catalyzed degradation of ethanol is also essential to the use of the catalyst in real-world applications. Increasing temperature from 25°C to 65°C caused a significant decrease in ethanol adsorption (47.1% loss in adsorption capacity); minimal changes in EtOH removal; and a dramatic increase in mineralization (37.3 vs. 74.8%), PCO rate (25.8 vs. 53.2 nM s^{-1}), and reaction quantum efficiency (42.7 vs. 82.5 nmol CO_2 μmol $photons^{-1}$). Intermediate evolution (acetaldehyde) in the effluent was also decreased. By elevating the reactor temperature to 45°C, a ~32% increase in reaction quantum efficiency was obtained over the use of UV-C irradiation at room temperature; this also allows for increased energy usage efficiency by utilizing both the light and heat energy of the UV-A light source. The positive effect of moderately increasing temperature can be explained by desorption of water from the catalyst, allowing for available active sites for target VOC degradation. Temperature can only be utilized to a maximum temperature (believed to occur near 65°C for the STC catalyst as displayed by the parabolic trends for PCO rate, mineralization, and reaction quantum efficiency. At higher temperatures, it is likely a loss of photo-generated charge carriers as described by Westrich et al[32].

Heightened relative humidity (RH) also caused a significant decrease (16.8 vs. 6.0 mg EtOH g $STCs^{-1}$) in ethanol adsorption and dark adsorption 95% breakthrough times (48.5 vs.16.8 hours), and correlated well with studies by Stokke and Mazyck[14] for methanol adsorption. In general, increased humidity was detrimental to PCO efficiency as mineralization, PCO rate, and reaction quantum efficiency were decreased while ACD evolution increased. While humidity

has the least impact on the PCO system (as seen by most trends following a natural log fit), the detrimental effect is due to a the competitive adsorption of water and target VOCs which inhibits oxidation and thus limits PCO efficiency as described by Fu et al[28]; for the STC catalyst, this adsorption inhibition appears to occur at reactive sites responsible for acetaldehyde oxidation rather than ethanol oxidation (increasing the intermediate evolution in the effluent).

Poisoning events included long-term exposure to low-VOC laboratory air and episodic spikes of either Freon 218 or hexamethylcyclotrisiloxane. To date, all poisoning studies have shown minimal (0-6%) decreases in PCO rates, mineralization, and minimal increases in ACD evolution, with little change in EtOH removal. These results, while studies are still ongoing, show great promise of this technology for use as part of a trace contaminant control system for niche applications such as air processing onboard the ISS or other new spacecrafts. The level of exposure seen in the ISS for Freon 218 and siloxanes is very low and would not likely cause critical failure of a PCO system in a short period of time. Continued low-level VOC exposure to the STC catalyst will allow for the continued evaluation of the lifetime of a possible PCO system for trace contaminant control. There still exist many other contaminants which may further impact the performance of this catalyst and require research; future studies are planned to measure the impact of both dichloromethane and xylene, much more recalcitrant compounds, on the efficiency of the catalyst.

APPENDIX: COPYRIGHT AGREEMENTS

ELSEVIER LICENSE
TERMS AND CONDITIONS

Jan 21, 2013

This is a License Agreement between Janelle L Coutts ("You") and Elsevier ("Elsevier") provided by Copyright Clearance Center ("CCC"). The license consists of your order details, the terms and conditions provided by Elsevier, and the payment terms and conditions.

All payments must be made in full to CCC. For payment instructions, please see information listed at the bottom of this form.

Supplier	Elsevier Limited The Boulevard,Langford Lane Kidlington,Oxford,OX5 1GB,UK
Registered Company Number	1982084
Customer name	Janelle L Coutts
Customer address	509 Alafaya Woods Blvd Apt E Oviedo, FL 32765
License number	3073770300100
License date	Jan 21, 2013
Licensed content publisher	Elsevier
Licensed content publication	Journal of Photochemistry and Photobiology A: Chemistry
Licensed content title	An overview of semiconductor photocatalysis
Licensed content author	Andrew Mills,Stephen Le Hunte
Licensed content date	31 July 1997
Licensed content volume number	108
Licensed content issue number	1
Number of pages	35
Start Page	1
End Page	35
Type of Use	reuse in a thesis/dissertation
Portion	figures/tables/illustrations
Number of figures/tables /illustrations	1
Format	both print and electronic
Are you the author of this Elsevier article?	No
Will you be translating?	No
Order reference number	

Title of your thesis/dissertation	TRACE CONTAMINANT CONTROL: AN IN-DEPTH STUDY OF A SILICA-TITANIA COMPOSITE FOR PHOTOCATALYTIC REMEDIATION OF CLOSED-ENIVRONMENT HABITAT AIR
Expected completion date	Feb 2013
Estimated size (number of pages)	80
Elsevier VAT number	GB 494 6272 12
Permissions price	0.00 USD
VAT/Local Sales Tax	0.0 USD / 0.0 GBP
Total	0.00 USD
Terms and Conditions	

INTRODUCTION

1. The publisher for this copyrighted material is Elsevier. By clicking "accept" in connection with completing this licensing transaction, you agree that the following terms and conditions apply to this transaction (along with the Billing and Payment terms and conditions established by Copyright Clearance Center, Inc. ("CCC"), at the time that you opened your Rightslink account and that are available at any time at http://myaccount.copyright.com).

GENERAL TERMS

2. Elsevier hereby grants you permission to reproduce the aforementioned material subject to the terms and conditions indicated.

3. Acknowledgement: If any part of the material to be used (for example, figures) has appeared in our publication with credit or acknowledgement to another source, permission must also be sought from that source. If such permission is not obtained then that material may not be included in your publication/copies. Suitable acknowledgement to the source must be made, either as a footnote or in a reference list at the end of your publication, as follows:

"Reprinted from Publication title, Vol /edition number, Author(s), Title of article / title of chapter, Pages No., Copyright (Year), with permission from Elsevier [OR APPLICABLE SOCIETY COPYRIGHT OWNER]." Also Lancet special credit - "Reprinted from The Lancet, Vol. number, Author(s), Title of article, Pages No., Copyright (Year), with permission from Elsevier."

4. Reproduction of this material is confined to the purpose and/or media for which permission is hereby given.

5. Altering/Modifying Material: Not Permitted. However figures and illustrations may be altered/adapted minimally to serve your work. Any other abbreviations, additions, deletions and/or any other alterations shall be made only with prior written authorization of Elsevier Ltd. (Please contact Elsevier at permissions@elsevier.com)

6. If the permission fee for the requested use of our material is waived in this instance, please be advised that your future requests for Elsevier materials may attract a fee.

7. Reservation of Rights: Publisher reserves all rights not specifically granted in the combination of (i) the license details provided by you and accepted in the course of this licensing transaction, (ii) these terms and conditions and (iii) CCC's Billing and Payment terms and conditions.

8. License Contingent Upon Payment: While you may exercise the rights licensed immediately upon issuance of the license at the end of the licensing process for the transaction, provided that you have disclosed complete and accurate details of your proposed use, no license is finally effective unless and until full payment is received from you (either by publisher or by CCC) as provided in CCC's Billing and Payment terms and conditions. If full payment is not received on a timely basis, then any license preliminarily granted shall be deemed automatically revoked and shall be void as if never granted. Further, in the event that you breach any of these terms and conditions or any of CCC's Billing and Payment terms and conditions, the license is automatically revoked and shall be void as if never granted. Use of materials as described in a revoked license, as well as any use of the materials beyond the scope of an unrevoked license, may constitute copyright infringement and publisher reserves the right to take any and all action to protect its copyright in the materials.

9. Warranties: Publisher makes no representations or warranties with respect to the licensed material.

10. Indemnity: You hereby indemnify and agree to hold harmless publisher and CCC, and their respective officers, directors, employees and agents, from and against any and all claims arising out of your use of the licensed material other than as specifically authorized pursuant to this license.

11. No Transfer of License: This license is personal to you and may not be sublicensed, assigned, or transferred by you to any other person without publisher's written permission.

12. No Amendment Except in Writing: This license may not be amended except in a writing signed by both parties (or, in the case of publisher, by CCC on publisher's behalf).

13. Objection to Contrary Terms: Publisher hereby objects to any terms contained in any purchase order, acknowledgment, check endorsement or other writing prepared by you, which terms are inconsistent with these terms and conditions or CCC's Billing and Payment terms and conditions. These terms and conditions, together with CCC's Billing and Payment terms and conditions (which are incorporated herein), comprise the entire agreement between you and publisher (and CCC) concerning this licensing transaction. In the event of any conflict between your obligations established by these terms and conditions and those established by CCC's Billing and Payment terms and conditions, these terms and conditions shall control.

14. Revocation: Elsevier or Copyright Clearance Center may deny the permissions described in this License at their sole discretion, for any reason or no reason, with a full refund payable to you. Notice of such denial will be made using the contact information provided by you. Failure to receive such notice will not alter or invalidate the denial. In no event will Elsevier or Copyright Clearance Center be responsible or liable for any costs, expenses or damage incurred by you as a result of a denial of your permission request, other than a refund of the

amount(s) paid by you to Elsevier and/or Copyright Clearance Center for denied permissions.

LIMITED LICENSE

The following terms and conditions apply only to specific license types:

15. **Translation:** This permission is granted for non-exclusive world **English** rights only unless your license was granted for translation rights. If you licensed translation rights you may only translate this content into the languages you requested. A professional translator must perform all translations and reproduce the content word for word preserving the integrity of the article. If this license is to re-use 1 or 2 figures then permission is granted for non-exclusive world rights in all languages.

16. **Website**: The following terms and conditions apply to electronic reserve and author websites:
Electronic reserve: If licensed material is to be posted to website, the web site is to be password-protected and made available only to bona fide students registered on a relevant course if:
This license was made in connection with a course,
This permission is granted for 1 year only. You may obtain a license for future website posting,
All content posted to the web site must maintain the copyright information line on the bottom of each image,
A hyper-text must be included to the Homepage of the journal from which you are licensing at http://www.sciencedirect.com/science/journal/xxxxx or the Elsevier homepage for books at http://www.elsevier.com , and
Central Storage: This license does not include permission for a scanned version of the material to be stored in a central repository such as that provided by Heron/XanEdu.

17. **Author website** for journals with the following additional clauses:

All content posted to the web site must maintain the copyright information line on the bottom of each image, and the permission granted is limited to the personal version of your paper. You are not allowed to download and post the published electronic version of your article (whether PDF or HTML, proof or final version), nor may you scan the printed edition to create an electronic version. A hyper-text must be included to the Homepage of the journal from which you are licensing at http://www.sciencedirect.com/science/journal/xxxxx . As part of our normal production process, you will receive an e-mail notice when your article appears on Elsevier's online service ScienceDirect (www.sciencedirect.com). That e-mail will include the article's Digital Object Identifier (DOI). This number provides the electronic link to the published article and should be included in the posting of your personal version. We ask that you wait until you receive this e-mail and have the DOI to do any posting.

Central Storage: This license does not include permission for a scanned version of the material to be stored in a central repository such as that provided by Heron/XanEdu.

18. **Author website** for books with the following additional clauses:
Authors are permitted to place a brief summary of their work online only.

A hyper-text must be included to the Elsevier homepage at http://www.elsevier.com . All content posted to the web site must maintain the copyright information line on the bottom of each image. You are not allowed to download and post the published electronic version of your chapter, nor may you scan the printed edition to create an electronic version.

Central Storage: This license does not include permission for a scanned version of the material to be stored in a central repository such as that provided by Heron/XanEdu.

19. **Website** (regular and for author): A hyper-text must be included to the Homepage of the journal from which you are licensing at http://www.sciencedirect.com/science/journal /xxxxx. or for books to the Elsevier homepage at http://www.elsevier.com

20. **Thesis/Dissertation**: If your license is for use in a thesis/dissertation your thesis may be submitted to your institution in either print or electronic form. Should your thesis be published commercially, please reapply for permission. These requirements include permission for the Library and Archives of Canada to supply single copies, on demand, of the complete thesis and include permission for UMI to supply single copies, on demand, of the complete thesis. Should your thesis be published commercially, please reapply for permission.

21. **Other Conditions:**

v1.6

If you would like to pay for this license now, please remit this license along with your payment made payable to "COPYRIGHT CLEARANCE CENTER" otherwise you will be invoiced within 48 hours of the license date. Payment should be in the form of a check or money order referencing your account number and this invoice number RLNK500938965.
Once you receive your invoice for this order, you may pay your invoice by credit card. Please follow instructions provided at that time.

Make Payment To:
Copyright Clearance Center
Dept 001
P.O. Box 843006
Boston, MA 02284-3006

For suggestions or comments regarding this order, contact RightsLink Customer Support: customercare@copyright.com or +1-877-622-5543 (toll free in the US) or +1-978-646-2777.

Gratis licenses (referencing $0 in the Total field) are free. Please retain this printable license for your reference. No payment is required.

ELSEVIER LICENSE
TERMS AND CONDITIONS

Feb 05, 2013

This is a License Agreement between Janelle L Coutts ("You") and Elsevier ("Elsevier") provided by Copyright Clearance Center ("CCC"). The license consists of your order details, the terms and conditions provided by Elsevier, and the payment terms and conditions.

All payments must be made in full to CCC. For payment instructions, please see information listed at the bottom of this form.

Supplier	Elsevier Limited The Boulevard,Langford Lane Kidlington,Oxford,OX5 1GB,UK
Registered Company Number	1982084
Customer name	Janelle L Coutts
Customer address	509 Alafaya Woods Blvd Apt E Oviedo, FL 32765
License number	3082471489004
License date	Feb 05, 2013
Licensed content publisher	Elsevier
Licensed content publication	Journal of Photochemistry and Photobiology A: Chemistry
Licensed content title	The effect of photon source on heterogeneous photocatalytic oxidation of ethanol by a silica–titania composite
Licensed content author	Janelle L. Coutts,Lanfang H. Levine,Jeffrey T. Richards,David W. Mazyck
Licensed content date	1 December 2011
Licensed content volume number	225
Licensed content issue number	1
Number of pages	7
Start Page	58
End Page	64
Type of Use	reuse in a thesis/dissertation
Intended publisher of new work	other
Portion	full article
Format	both print and electronic
Are you the author of this Elsevier article?	Yes
Will you be translating?	No

Order reference number	
Title of your thesis/dissertation	TRACE CONTAMINANT CONTROL: AN IN-DEPTH STUDY OF A SILICA-TITANIA COMPOSITE FOR PHOTOCATALYTIC REMEDIATION OF CLOSED-ENIVRONMENT HABITAT AIR
Expected completion date	Feb 2013
Estimated size (number of pages)	80
Elsevier VAT number	GB 494 6272 12
Permissions price	0.00 USD
VAT/Local Sales Tax	0.0 USD / 0.0 GBP
Total	0.00 USD
Terms and Conditions	

INTRODUCTION

1. The publisher for this copyrighted material is Elsevier. By clicking "accept" in connection with completing this licensing transaction, you agree that the following terms and conditions apply to this transaction (along with the Billing and Payment terms and conditions established by Copyright Clearance Center, Inc. ("CCC"), at the time that you opened your Rightslink account and that are available at any time at http://myaccount.copyright.com).

GENERAL TERMS

2. Elsevier hereby grants you permission to reproduce the aforementioned material subject to the terms and conditions indicated.

3. Acknowledgement: If any part of the material to be used (for example, figures) has appeared in our publication with credit or acknowledgement to another source, permission must also be sought from that source. If such permission is not obtained then that material may not be included in your publication/copies. Suitable acknowledgement to the source must be made, either as a footnote or in a reference list at the end of your publication, as follows:

"Reprinted from Publication title, Vol /edition number, Author(s), Title of article / title of chapter, Pages No., Copyright (Year), with permission from Elsevier [OR APPLICABLE SOCIETY COPYRIGHT OWNER]." Also Lancet special credit - "Reprinted from The Lancet, Vol. number, Author(s), Title of article, Pages No., Copyright (Year), with permission from Elsevier."

4. Reproduction of this material is confined to the purpose and/or media for which permission is hereby given.

5. Altering/Modifying Material: Not Permitted. However figures and illustrations may be altered/adapted minimally to serve your work. Any other abbreviations, additions, deletions and/or any other alterations shall be made only with prior written authorization of Elsevier Ltd. (Please contact Elsevier at permissions@elsevier.com)

6. If the permission fee for the requested use of our material is waived in this instance, please

be advised that your future requests for Elsevier materials may attract a fee.

7. Reservation of Rights: Publisher reserves all rights not specifically granted in the combination of (i) the license details provided by you and accepted in the course of this licensing transaction, (ii) these terms and conditions and (iii) CCC's Billing and Payment terms and conditions.

8. License Contingent Upon Payment: While you may exercise the rights licensed immediately upon issuance of the license at the end of the licensing process for the transaction, provided that you have disclosed complete and accurate details of your proposed use, no license is finally effective unless and until full payment is received from you (either by publisher or by CCC) as provided in CCC's Billing and Payment terms and conditions. If full payment is not received on a timely basis, then any license preliminarily granted shall be deemed automatically revoked and shall be void as if never granted. Further, in the event that you breach any of these terms and conditions or any of CCC's Billing and Payment terms and conditions, the license is automatically revoked and shall be void as if never granted. Use of materials as described in a revoked license, as well as any use of the materials beyond the scope of an unrevoked license, may constitute copyright infringement and publisher reserves the right to take any and all action to protect its copyright in the materials.

9. Warranties: Publisher makes no representations or warranties with respect to the licensed material.

10. Indemnity: You hereby indemnify and agree to hold harmless publisher and CCC, and their respective officers, directors, employees and agents, from and against any and all claims arising out of your use of the licensed material other than as specifically authorized pursuant to this license.

11. No Transfer of License: This license is personal to you and may not be sublicensed, assigned, or transferred by you to any other person without publisher's written permission.

12. No Amendment Except in Writing: This license may not be amended except in a writing signed by both parties (or, in the case of publisher, by CCC on publisher's behalf).

13. Objection to Contrary Terms: Publisher hereby objects to any terms contained in any purchase order, acknowledgment, check endorsement or other writing prepared by you, which terms are inconsistent with these terms and conditions or CCC's Billing and Payment terms and conditions. These terms and conditions, together with CCC's Billing and Payment terms and conditions (which are incorporated herein), comprise the entire agreement between you and publisher (and CCC) concerning this licensing transaction. In the event of any conflict between your obligations established by these terms and conditions and those established by CCC's Billing and Payment terms and conditions, these terms and conditions shall control.

14. Revocation: Elsevier or Copyright Clearance Center may deny the permissions described in this License at their sole discretion, for any reason or no reason, with a full refund payable to you. Notice of such denial will be made using the contact information provided by you. Failure to receive such notice will not alter or invalidate the denial. In no event will Elsevier or Copyright Clearance Center be responsible or liable for any costs, expenses or damage

incurred by you as a result of a denial of your permission request, other than a refund of the amount(s) paid by you to Elsevier and/or Copyright Clearance Center for denied permissions.

LIMITED LICENSE

The following terms and conditions apply only to specific license types:

15. **Translation**: This permission is granted for non-exclusive world **English** rights only unless your license was granted for translation rights. If you licensed translation rights you may only translate this content into the languages you requested. A professional translator must perform all translations and reproduce the content word for word preserving the integrity of the article. If this license is to re-use 1 or 2 figures then permission is granted for non-exclusive world rights in all languages.

16. **Website**: The following terms and conditions apply to electronic reserve and author websites:
Electronic reserve: If licensed material is to be posted to website, the web site is to be password-protected and made available only to bona fide students registered on a relevant course if:
This license was made in connection with a course,
This permission is granted for 1 year only. You may obtain a license for future website posting,
All content posted to the web site must maintain the copyright information line on the bottom of each image,
A hyper-text must be included to the Homepage of the journal from which you are licensing at http://www.sciencedirect.com/science/journal/xxxxx or the Elsevier homepage for books at http://www.elsevier.com , and
Central Storage: This license does not include permission for a scanned version of the material to be stored in a central repository such as that provided by Heron/XanEdu.

17. **Author website** for journals with the following additional clauses:

All content posted to the web site must maintain the copyright information line on the bottom of each image, and the permission granted is limited to the personal version of your paper. You are not allowed to download and post the published electronic version of your article (whether PDF or HTML, proof or final version), nor may you scan the printed edition to create an electronic version. A hyper-text must be included to the Homepage of the journal from which you are licensing at http://www.sciencedirect.com/science/journal/xxxxx . As part of our normal production process, you will receive an e-mail notice when your article appears on Elsevier's online service ScienceDirect (www.sciencedirect.com). That e-mail will include the article's Digital Object Identifier (DOI). This number provides the electronic link to the published article and should be included in the posting of your personal version. We ask that you wait until you receive this e-mail and have the DOI to do any posting.

Central Storage: This license does not include permission for a scanned version of the material to be stored in a central repository such as that provided by Heron/XanEdu.

18. **Author website** for books with the following additional clauses:

Authors are permitted to place a brief summary of their work online only.
A hyper-text must be included to the Elsevier homepage at http://www.elsevier.com . All content posted to the web site must maintain the copyright information line on the bottom of each image. You are not allowed to download and post the published electronic version of your chapter, nor may you scan the printed edition to create an electronic version.

Central Storage: This license does not include permission for a scanned version of the material to be stored in a central repository such as that provided by Heron/XanEdu.

19. **Website** (regular and for author): A hyper-text must be included to the Homepage of the journal from which you are licensing at http://www.sciencedirect.com/science/journal /xxxxx. or for books to the Elsevier homepage at http://www.elsevier.com

20. **Thesis/Dissertation**: If your license is for use in a thesis/dissertation your thesis may be submitted to your institution in either print or electronic form. Should your thesis be published commercially, please reapply for permission. These requirements include permission for the Library and Archives of Canada to supply single copies, on demand, of the complete thesis and include permission for UMI to supply single copies, on demand, of the complete thesis. Should your thesis be published commercially, please reapply for permission.

21. **Other Conditions**:

v1.6

If you would like to pay for this license now, please remit this license along with your payment made payable to "COPYRIGHT CLEARANCE CENTER" otherwise you will be invoiced within 48 hours of the license date. Payment should be in the form of a check or money order referencing your account number and this invoice number RLNK500950154.
Once you receive your invoice for this order, you may pay your invoice by credit card. Please follow instructions provided at that time.

Make Payment To:
Copyright Clearance Center
Dept 001
P.O. Box 843006
Boston, MA 02284-3006

For suggestions or comments regarding this order, contact RightsLink Customer Support: customercare@copyright.com or +1-877-622-5543 (toll free in the US) or +1-978-646-2777.

Gratis licenses (referencing $0 in the Total field) are free. Please retain this printable license for your reference. No payment is required.

ELSEVIER LICENSE
TERMS AND CONDITIONS

Feb 05, 2013

This is a License Agreement between Janelle L Coutts ("You") and Elsevier ("Elsevier") provided by Copyright Clearance Center ("CCC"). The license consists of your order details, the terms and conditions provided by Elsevier, and the payment terms and conditions.

All payments must be made in full to CCC. For payment instructions, please see information listed at the bottom of this form.

Supplier	Elsevier Limited The Boulevard,Langford Lane Kidlington,Oxford,OX5 1GB,UK
Registered Company Number	1982084
Customer name	Janelle L Coutts
Customer address	509 Alafaya Woods Blvd Apt E Oviedo, FL 32765
License number	3082480218732
License date	Feb 05, 2013
Licensed content publisher	Elsevier
Licensed content publication	Journal of Catalysis
Licensed content title	Mechanism of the Photocatalytic Oxidation of Ethanol on TiO2
Licensed content author	Darrin S Muggli,Justin T McCue,John L Falconer
Licensed content date	25 January 1998
Licensed content volume number	173
Licensed content issue number	2
Number of pages	14
Start Page	470
End Page	483
Type of Use	reuse in a thesis/dissertation
Intended publisher of new work	other
Portion	figures/tables/illustrations
Number of figures/tables /illustrations	1
Format	both print and electronic
Are you the author of this Elsevier article?	No
Will you be translating?	No

Order reference number	
Title of your thesis/dissertation	TRACE CONTAMINANT CONTROL: AN IN-DEPTH STUDY OF A SILICA-TITANIA COMPOSITE FOR PHOTOCATALYTIC REMEDIATION OF CLOSED-ENIVRONMENT HABITAT AIR
Expected completion date	Feb 2013
Estimated size (number of pages)	80
Elsevier VAT number	GB 494 6272 12
Permissions price	0.00 USD
VAT/Local Sales Tax	0.0 USD / 0.0 GBP
Total	0.00 USD
Terms and Conditions	

INTRODUCTION

1. The publisher for this copyrighted material is Elsevier. By clicking "accept" in connection with completing this licensing transaction, you agree that the following terms and conditions apply to this transaction (along with the Billing and Payment terms and conditions established by Copyright Clearance Center, Inc. ("CCC"), at the time that you opened your Rightslink account and that are available at any time at http://myaccount.copyright.com).

GENERAL TERMS

2. Elsevier hereby grants you permission to reproduce the aforementioned material subject to the terms and conditions indicated.

3. Acknowledgement: If any part of the material to be used (for example, figures) has appeared in our publication with credit or acknowledgement to another source, permission must also be sought from that source. If such permission is not obtained then that material may not be included in your publication/copies. Suitable acknowledgement to the source must be made, either as a footnote or in a reference list at the end of your publication, as follows:

"Reprinted from Publication title, Vol /edition number, Author(s), Title of article / title of chapter, Pages No., Copyright (Year), with permission from Elsevier [OR APPLICABLE SOCIETY COPYRIGHT OWNER]." Also Lancet special credit - "Reprinted from The Lancet, Vol. number, Author(s), Title of article, Pages No., Copyright (Year), with permission from Elsevier."

4. Reproduction of this material is confined to the purpose and/or media for which permission is hereby given.

5. Altering/Modifying Material: Not Permitted. However figures and illustrations may be altered/adapted minimally to serve your work. Any other abbreviations, additions, deletions and/or any other alterations shall be made only with prior written authorization of Elsevier Ltd. (Please contact Elsevier at permissions@elsevier.com)

6. If the permission fee for the requested use of our material is waived in this instance, please

be advised that your future requests for Elsevier materials may attract a fee.

7. Reservation of Rights: Publisher reserves all rights not specifically granted in the combination of (i) the license details provided by you and accepted in the course of this licensing transaction, (ii) these terms and conditions and (iii) CCC's Billing and Payment terms and conditions.

8. License Contingent Upon Payment: While you may exercise the rights licensed immediately upon issuance of the license at the end of the licensing process for the transaction, provided that you have disclosed complete and accurate details of your proposed use, no license is finally effective unless and until full payment is received from you (either by publisher or by CCC) as provided in CCC's Billing and Payment terms and conditions. If full payment is not received on a timely basis, then any license preliminarily granted shall be deemed automatically revoked and shall be void as if never granted. Further, in the event that you breach any of these terms and conditions or any of CCC's Billing and Payment terms and conditions, the license is automatically revoked and shall be void as if never granted. Use of materials as described in a revoked license, as well as any use of the materials beyond the scope of an unrevoked license, may constitute copyright infringement and publisher reserves the right to take any and all action to protect its copyright in the materials.

9. Warranties: Publisher makes no representations or warranties with respect to the licensed material.

10. Indemnity: You hereby indemnify and agree to hold harmless publisher and CCC, and their respective officers, directors, employees and agents, from and against any and all claims arising out of your use of the licensed material other than as specifically authorized pursuant to this license.

11. No Transfer of License: This license is personal to you and may not be sublicensed, assigned, or transferred by you to any other person without publisher's written permission.

12. No Amendment Except in Writing: This license may not be amended except in a writing signed by both parties (or, in the case of publisher, by CCC on publisher's behalf).

13. Objection to Contrary Terms: Publisher hereby objects to any terms contained in any purchase order, acknowledgment, check endorsement or other writing prepared by you, which terms are inconsistent with these terms and conditions or CCC's Billing and Payment terms and conditions. These terms and conditions, together with CCC's Billing and Payment terms and conditions (which are incorporated herein), comprise the entire agreement between you and publisher (and CCC) concerning this licensing transaction. In the event of any conflict between your obligations established by these terms and conditions and those established by CCC's Billing and Payment terms and conditions, these terms and conditions shall control.

14. Revocation: Elsevier or Copyright Clearance Center may deny the permissions described in this License at their sole discretion, for any reason or no reason, with a full refund payable to you. Notice of such denial will be made using the contact information provided by you. Failure to receive such notice will not alter or invalidate the denial. In no event will Elsevier or Copyright Clearance Center be responsible or liable for any costs, expenses or damage

incurred by you as a result of a denial of your permission request, other than a refund of the amount(s) paid by you to Elsevier and/or Copyright Clearance Center for denied permissions.

LIMITED LICENSE

The following terms and conditions apply only to specific license types:

15. **Translation**: This permission is granted for non-exclusive world **English** rights only unless your license was granted for translation rights. If you licensed translation rights you may only translate this content into the languages you requested. A professional translator must perform all translations and reproduce the content word for word preserving the integrity of the article. If this license is to re-use 1 or 2 figures then permission is granted for non-exclusive world rights in all languages.

16. **Website**: The following terms and conditions apply to electronic reserve and author websites:
Electronic reserve: If licensed material is to be posted to website, the web site is to be password-protected and made available only to bona fide students registered on a relevant course if:
This license was made in connection with a course,
This permission is granted for 1 year only. You may obtain a license for future website posting,
All content posted to the web site must maintain the copyright information line on the bottom of each image,
A hyper-text must be included to the Homepage of the journal from which you are licensing at http://www.sciencedirect.com/science/journal/xxxxx or the Elsevier homepage for books at http://www.elsevier.com , and
Central Storage: This license does not include permission for a scanned version of the material to be stored in a central repository such as that provided by Heron/XanEdu.

17. **Author website** for journals with the following additional clauses:

All content posted to the web site must maintain the copyright information line on the bottom of each image, and the permission granted is limited to the personal version of your paper. You are not allowed to download and post the published electronic version of your article (whether PDF or HTML, proof or final version), nor may you scan the printed edition to create an electronic version. A hyper-text must be included to the Homepage of the journal from which you are licensing at http://www.sciencedirect.com/science/journal/xxxxx . As part of our normal production process, you will receive an e-mail notice when your article appears on Elsevier's online service ScienceDirect (www.sciencedirect.com). That e-mail will include the article's Digital Object Identifier (DOI). This number provides the electronic link to the published article and should be included in the posting of your personal version. We ask that you wait until you receive this e-mail and have the DOI to do any posting.

Central Storage: This license does not include permission for a scanned version of the material to be stored in a central repository such as that provided by Heron/XanEdu.

18. **Author website** for books with the following additional clauses:

Authors are permitted to place a brief summary of their work online only.
A hyper-text must be included to the Elsevier homepage at http://www.elsevier.com . All content posted to the web site must maintain the copyright information line on the bottom of each image. You are not allowed to download and post the published electronic version of your chapter, nor may you scan the printed edition to create an electronic version.

Central Storage: This license does not include permission for a scanned version of the material to be stored in a central repository such as that provided by Heron/XanEdu.

19. **Website** (regular and for author): A hyper-text must be included to the Homepage of the journal from which you are licensing at http://www.sciencedirect.com/science/journal /xxxxx. or for books to the Elsevier homepage at http://www.elsevier.com

20. **Thesis/Dissertation**: If your license is for use in a thesis/dissertation your thesis may be submitted to your institution in either print or electronic form. Should your thesis be published commercially, please reapply for permission. These requirements include permission for the Library and Archives of Canada to supply single copies, on demand, of the complete thesis and include permission for UMI to supply single copies, on demand, of the complete thesis. Should your thesis be published commercially, please reapply for permission.

21. **Other Conditions**:

v1.6

If you would like to pay for this license now, please remit this license along with your payment made payable to "COPYRIGHT CLEARANCE CENTER" otherwise you will be invoiced within 48 hours of the license date. Payment should be in the form of a check or money order referencing your account number and this invoice number RLNK500950161.
Once you receive your invoice for this order, you may pay your invoice by credit card. Please follow instructions provided at that time.

Make Payment To:
Copyright Clearance Center
Dept 001
P.O. Box 843006
Boston, MA 02284-3006

For suggestions or comments regarding this order, contact RightsLink Customer Support: customercare@copyright.com or +1-877-622-5543 (toll free in the US) or +1-978-646-2777.

Gratis licenses (referencing $0 in the Total field) are free. Please retain this printable license for your reference. No payment is required.

REFERENCES

[1] J. Zhao, X. Yang, Photocatalytic oxidation for indoor air purification: a literature review, Building and Environment, 38 (2003) 645-654.

[2] E. Uhde, in: T. Salthammer (Ed.) Organic Indoor Air Pollutants: Occurrence, Measurement, Evaluation, Wiley-VCH, Wienheim, Germany, 1999, pp. 3-14.

[3] H.T. Corporation, Thermal and Catalytic Oxidizers: Gas and Electric Fired Systems Specifications Sheets, in, Flemington, NJ.

[4] A.S.K. Warahena, Y.K. Chuah, Energy Recovery Efficiency and Cost Analysis of VOC Thermal Oxidation Pollution Control Technology, Environmental Science & Technology, 43 (2009) 6101-6105.

[5] C.W. Babbitt, J.M. Stokke, D.W. Mazyck, A.S. Lindner, Design-based life cycle assessment of hazardous air pollutant control options at pulp and paper mills: a comparison of thermal oxidation to photocatalytic oxidation and biofiltration, Journal of Chemical Technology & Biotechnology, 84 (2009) 725-737.

[6] M.R. Hoffmann, S.T. Martin, W. Choi, D.W. Bahnemann, Environmental Applications of Semiconductor Photocatalysis, Chemical Reviews, 95 (1995) 69-96.

[7] J. Mo, Y. Zhang, Q. Xu, J.J. Lamson, R. Zhao, Photocatalytic purification of volatile organic compounds in indoor air: A literature review, Atmospheric Environment, 43 (2009) 2229-2246.

[8] J.L. Coutts, L.H. Levine, J.T. Richards, D.W. Mazyck, The effect of photon source on heterogeneous photocatalytic oxidation of ethanol by a silica–titania composite, Journal of Photochemistry and Photobiology A: Chemistry, 225 (2011) 58-64.

[9] O. Carp, C.L. Huisman, A. Reller, Photoinduced reactivity of titanium dioxide, Progress in Solid State Chemistry, 32 (2004) 33-177.

[10] A. Mills, S. Le Hunte, An overview of semiconductor photocatalysis, Journal of Photochemistry and Photobiology A: Chemistry, 108 (1997) 1-35.

[11] B. Ohtani, O.O. Prieto-Mahaney, D. Li, R. Abe, What is Degussa (Evonik) P25? Crystalline composition analysis, reconstruction from isolated pure particles and photocatalytic activity test, Journal of Photochemistry and Photobiology A: Chemistry, 216 (2010) 179-182.

[12] Y. Luo, D.F. Ollis, Heterogeneous Photocatalytic Oxidation of Trichloroethylene and Toluene Mixtures in Air: Kinetic Promotion and Inhibition, Time-Dependent Catalyst Activity, Journal of Catalysis, 163 (1996) 1-11.

[13] J. M. Stokke, D.W. Mazyck, C.Y. Wu, R. Sheahan, Photocatalytic oxidation of methanol using silica-titania composites in a packed-bed reactor, Environmental Progress, 25 (2006) 312-318.

[14] J.M. Stokke, D.W. Mazyck, Photocatalytic Degradation of Methanol Using Silica–Titania Composite Pellets: Effect of Pore Size on Mass Transfer and Reaction Kinetics, Environmental Science & Technology, 42 (2008) 3808-3813.

[15] L.H. Levine, J.T. Richards, J.L. Coutts, R. Soler, F. Maxik, R.M. Wheeler, Feasibility of Ultraviolet-Light-Emitting Diodes as an Alternative Light Source for Photocatalysis, Journal of the Air & Waste Management Association (Air & Waste Management Association), 61 (2011) 932-940.

[16] S. Kwon, M. Fan, A.T. Cooper, Photocatalytic Applications of Micro- and Nano-TiO2 in Environmental Engineering, Critical Reviews in Environmental Science and Technology, 38 (2008) 197-226.

[17] A.G. Agrios, K.A. Gray, E. Weitz, Photocatalytic Transformation of 2,4,5-Trichlorophenol on TiO2 under Sub-Band-Gap Illumination, Langmuir, 19 (2003) 1402-1409.

[18] M.L. Sauer, D.F. Ollis, Photocatalyzed Oxidation of Ethanol and Acetaldehyde in Humidified Air, Journal of Catalysis, 158 (1996) 570-582.

[19] M.R. Nimlos, E.J. Wolfrum, M.L. Brewer, J.A. Fennell, G. Bintner, Gas-Phase Heterogeneous Photocatalytic Oxidation of Ethanol: Pathways and Kinetic Modeling, Environmental Science & Technology, 30 (1996) 3102-3110.

[20] D.S. Muggli, J.T. McCue, J.L. Falconer, Mechanism of the Photocatalytic Oxidation of Ethanol on TiO2, Journal of Catalysis, 173 (1998) 470-483.

[21] M.F.J. Dijkstra, H.J. Panneman, J.G.M. Winkelman, J.J. Kelly, A.A.C.M. Beenackers, Modeling the photocatalytic degradation of formic acid in a reactor with immobilized catalyst, Chemical Engineering Science, 57 (2002) 4895-4907.

[22] J. Cen, X. Li, M. He, S. Zheng, M. Feng, The effect of background irradiation on photocatalytic efficiencies of TiO2 thin films, Chemosphere, 62 (2006) 810-816.

[23] R.M. Alberici, W.F. Jardim, Photocatalytic destruction of VOCs in the gas-phase using titanium dioxide, Applied Catalysis B: Environmental, 14 (1997) 55-68.

[24] S.B. Kim, S.C. Hong, Kinetic study for photocatalytic degradation of volatile organic compounds in air using thin film TiO2 photocatalyst, Applied Catalysis B: Environmental, 35 (2002) 305-315.

[25] W.A. Jacoby, Destruction of Trichloroethylene in Air Via Semiconductor Mediated Gas-solid Heterogeneous Photocatalysis, University Microfilms Int./UMI, 1994.

[26] M.A. Grela, A.J. Colussi, Photon Energy and Photon Intermittence Effects on the Quantum Efficiency of Photoinduced Oxidations in Crystalline and Metastable TiO2 Colloidal Nanoparticles, The Journal of Physical Chemistry B, 103 (1999) 2614-2619.

[27] A. Sandhu, The future of ultraviolet LEDs, Nature Photonics, 1 (2007).

[28] X. Fu, L.A. Clark, W.A. Zeltner, M.A. Anderson, Effects of reaction temperature and water vapor content on the heterogeneous photocatalytic oxidation of ethylene, Journal of Photochemistry and Photobiology A: Chemistry, 97 (1996) 181-186.

[29] N.R. Blake, G.L. Griffin, Selectivity control during the photoassisted oxidation of 1-butanol on titanium dioxide, The Journal of Physical Chemistry, 92 (1988) 5697-5701.

[30] P. Pichat, J.M. Herrmann, J. Disdier, M.N. Mozzanega, Photocatalytic oxidation of propene over various oxides at 320 K. Selectivity, The Journal of Physical Chemistry, 83 (1979) 3122-3126.

[31] S.Y.-N. M.A. Anderson, S. Cervera-March, in: H.A.-E. D.F. Ollis (Ed.) Photocatalytic Purification and Treatment of Water and Air, Elsevier, Amsterdam, 1993, pp. 777-782.

[32] T.A. Westrich, K.A. Dahlberg, M. Kaviany, J.W. Schwank, High-Temperature Photocatalytic Ethylene Oxidation over TiO2, The Journal of Physical Chemistry C, 115 (2011) 16537-16543.

[33] C. Stavrakakis, C. Raillard, cile, V. quet, rie, P. Le Cloirec, TiO2-Based Materials for Toluene Photocalytic Oxidation: Water Vapor Influence, Journal of Advanced Oxidation Technologies, 10 (2007) 94-100.

[34] T. Ibusuki, K. Takeuchi, Toluene oxidation on u.v.-irradiated titanium dioxide with and without O2, NO2 OR H2O at ambient temperature, Atmospheric Environment (1967), 20 (1986) 1711-1715.

[35] P.B. Amama, K. Itoh, M. Murabayashi, Photocatalytic oxidation of trichloroethylene in humidified atmosphere, Journal of Molecular Catalysis A: Chemical, 176 (2001) 165-172.

[36] J. Peral, D.F. Ollis, Heterogeneous photocatalytic oxidation of gas-phase organics for air purification: Acetone, 1-butanol, butyraldehyde, formaldehyde, and m-xylene oxidation, Journal of Catalysis, 136 (1992) 554-565.

[37] J.L. Perry, A Design Basis for Spacecraft Cabin Trace Contaminant Control, in: International Conference on Environmental Systems, SAE International, Savannah, GA, 2009.

[38] S.O. Hay, T.N. Obee, C. Thibaud-Erkey, The deactivation of photocatalytic based air purifiers by ambient siloxanes, Applied Catalysis B: Environmental, 99 (2010) 435-441.

[39] R.-D. Sun, A. Nakajima, T. Watanabe, K. Hashimoto, Decomposition of gas-phase octamethyltrisiloxane on TiO2 thin film photocatalysts—catalytic activity, deactivation, and regeneration, Journal of Photochemistry and Photobiology A: Chemistry, 154 (2003) 203-209.

[40] A.V.P. Macatangay, Jay L.; Belcher, Paul L.; Johnson, Sharon A., Status of the International Space Station (ISS) Trace Contaminant Control System, in: International Conference on Environmental Systems, SAE International, Savannah, GA, 2009.

[41] S. Karmakar, H.L. Greene, An Investigation of CFC12 (CCl2F2) Decomposition on TiO2 Catalyst, Journal of Catalysis, 151 (1995) 394-406.

[42] M.M. Farris, A.A. Klinghoffer, J.A. RosSnl, D.E. Tevault, Deactivation of a Pt/Al2O3 catalyst during the oxidation of hexafluoropropylene, Catalysis Today, 11 (1992) 501-516.

[43] K. Tennakone, K.G.U. Wijayantha, Photocatalysis of CFC degradation by titanium dioxide, Applied Catalysis B: Environmental, 57 (2005) 9-12.

[44] B. Sangchakr, T. Hisanaga, K. Tanaka, Photocatalytic degradation of 1,1-difluoroethane (HFC - 152a), Chemosphere, 36 (1998) 1985-1992.

[45] T.A.K. Egerton, C. J., The influence of llight intensity on photoactivity of TiO_2 pigmented systems, Journal of the Oil and Colour Chemists' Association, 62 (1979) 386-391.

[46] M.A. Grela, M.A. Brusa, A.J. Colussi, Harnessing Excess Photon Energy in Photoinduced Surface Electron Transfer between Salicylate and Illuminated Titanium Dioxide Nanoparticles, The Journal of Physical Chemistry B, 101 (1997) 10986-10989.

[47] Y. Paz, Photocatalytic Treatment of Air: From Basic Aspects to Reactors, in: I.d.L. Hugo, R. Benito Serrano (Eds.) Advances in Chemical Engineering, Academic Press, 2009, pp. 289-336.

[48] D.W.M. Jennifer M. Stokke, Effect of Catalyst Support on Photocatalytic Destruction of VOCs in a Packed-Bed Reactor, in: International Conference on Environmental Systems, SAE International, Chicago, IL, 2007.